THE ASTROPHYSICAL JOURNAL, 356:432–455, 1990 June 20

A STUDY OF BL LACERTAE–TYPE OBJECTS WITH *EXOSAT*. I. FLUX CORRELATIONS, LUMINOSITY VARIABILITY, AND SPECTRAL VARIABILITY

P. GIOMMI,[1,2] P. BARR,[1] B. GARILLI,[3] D. MACCAGNI,[3] AND A. M. T. POLLOCK[1]

Received 1989 August 21; accepted 1989 December 14

ABSTRACT

Results are presented from a uniform and systematic analysis of more than 200 X-ray observations of 36 BL Lacertae objects obtained from the *EXOSAT* archive. All but two objects were detected at least once. Strong luminosity variability, which reached a factor of 30 in one case, was a common property of these objects. Variability was usually more pronounced in the hard (0.7–8 keV) X-ray energy band than in soft X-rays, implying hardening of the spectrum as the sources brightened. This behavior is opposite to that observed in some Seyfert galaxies. Four objects (ON 325, 1E 1402.3+0416, PKS 2005−489, PKS 2155−304) showed large-amplitude flux variations on time scales of a few hours. In addition, 1H 0414+009, PKS 0548−322, Mrk 421, and Mrk 501 changed their intensity by ≈20%–40% on the same time scale.

There were no long-term trends in the X-ray emission of any of the objects that were well monitored over a long period of time. The commonest form of variability in the soft X-ray band can be represented by small-amplitude variations about a quiescent level that remains approximately constant for years. A statistical analysis shows that, on average, BL Lacs spend less than 10% of the time in flares that involve luminosity variations of factors of 2 or more.

The α_{ox}-α_{ro} diagram of the objects in the sample allows the identification of two subclasses of BL Lacs characterized by different intrinsic properties, namely, the Q–BL Lacs, which include most of the classical radio-selected objects and show energy distributions similar to those of other radio-loud active galactic nuclei, and the X–BL Lacs, which include all the optically and X-ray discovered objects. X–BL Lacs probably constitute the predominant population.

There were no obvious differences in the X-ray variability properties of the two subclasses.

Analysis of the soft X-ray emission reveals no evidence for intrinsic absorption in excess of a few times 10^{20} atoms cm^{-2} in any of the objects for which data of sufficiently good quality were available.

Subject headings: BL Lacertae objects — galaxies: X-rays — X-rays: sources

I. INTRODUCTION

BL Lacertae–type objects are a class of extragalactic sources characterized by the absence of optical emission lines, by large amplitude and rapid flux variability, and by the polarization of their radio and/or optical flux (Stein, O'Dell, and Strittmatter 1976). BL Lac objects exhibit many of the properties typical of other types of active galactic nuclei (AGNs), although they also differ in several ways. BL Lacs are among the most variable extragalactic objects known at all frequencies. They show neither broad emission lines (by definition), although in some cases emission lines have been observed during periods of low activity (e.g., Burbidge and Hewitt 1987), nor the excess emission in the blue/ultraviolet part of the spectrum, the so-called blue bump, which is instead a characteristic feature of QSOs and Seyfert galaxies. Their cosmological evolution and X-ray luminosity function also seem to be different from those of other AGNs (Maccacaro *et al.* 1984; Maccacaro *et al.* 1989; Giommi *et al.* 1989*a*). Their radio through X-ray energy distribution is smooth, with most of the luminosity emitted between the infrared and the UV part of the spectrum. To date there are no examples of BL Lac objects with undetectable radio emission (Stocke *et al.* 1990). Finally, because of the lack of emission lines, the redshifts of several BL Lacs are not known.

BL Lac objects are rare and make up only about 2% of all known AGNs. Although they were discovered some 20 years ago (Schmitt 1968), so far only a few dozen have been found (Burbidge and Hewitt 1987). In contrast, a few thousand QSOs appear in recent catalogs of AGNs (e.g., Hewitt and Burbidge 1987; Véron-Cetty and Véron 1985).

Traditionally, BL Lacs have been discovered in high-frequency radio surveys. These objects are often referred to as radio-selected BL Lacs. Attempts to search for BL Lacs at optical frequencies, through multicolor selection or polarization surveys, have so far produced disappointing results (Impey and Brand 1982; Borra and Corriveau 1984; Jannuzi and Green 1989). An efficient method of discovering BL Lacs has recently become available and consists in the optical identification of sources discovered in X-ray surveys (e.g., Stocke *et al.* 1988). BL Lacertae objects discovered in this way are commonly known as X-ray–selected BL Lacs. About 20% of the X-ray–selected AGNs with flux in excess of $\approx 10^{-12}$ ergs cm^{-2} s^{-1}, in the 1–6 keV band, are BL Lacs (Piccinotti *et al.* 1982; Stocke *et al.* 1988). Recently, Maccacaro *et al.* (1989) reported the discovery of about 30 new X-ray–selected BL Lacs among the sources of the *Einstein* Extended Medium-Sensitivity Survey (EMSS; Gioia *et al.* 1990), which covers about 3% of the high Galactic latitude sky. A similar number of BL Lacs have recently been discovered in the *EXOSAT* High Galactic Latitude Survey (HGLS; Giommi, Tagliaferri, and Angelini

[1] *EXOSAT* Observatory, Astrophysics Division, Space Science Department of ESA, ESTEC, The Netherlands.
[2] On leave of absence from CNR, Istituto di Fisica Cosmica, Milano, Italy.
[3] Istituto di Fisica Cosmica del CNR, Milano Italy.

1988; Giommi *et al.* 1989*a*, *b*; Tagliaferri *et al.* 1989*a*) and among the sources detected with the A-1 and A-3 experiments of the *HEAO 1* satellite (Remillard *et al.* 1989; Bradt *et al.* 1988; Schwartz *et al.* 1989).

Ledden and O'Dell (1985), on the grounds of the very small number of X-ray-selected BL Lacs then known, concluded that these sources represent a minority among the population of BL Lac objects. Recent findings, however, suggest instead that X-ray-selected sources may be the dominant component (e.g., Maraschi *et al.* 1986).

II. THE SAMPLE

We have considered all the BL Lac objects that are listed in the catalog of Burbidge and Hewitt (1987) that were observed at least once with the low-energy (LE) and medium-energy (ME) instruments aboard *EXOSAT* (see Taylor *et al.* 1981 and White and Peacock 1988 for a description), with the addition of two objects, H1427+42 and 4U 1722+11, which have recently been classified as BL Lacs by Remillard *et al.* (1989) and Griffiths *et al.* (1989). The sample thus defined includes 36 objects.

All data were obtained from the *EXOSAT* archive. A good fraction of the *EXOSAT* data on BL Lacertae objects have been analyzed and published by the original *EXOSAT* observers (e.g., Morini *et al.* 1986; Staubert, Brunner, and Worrall 1986; Staubert *et al.* 1986; Brown *et al.* 1986; Giommi *et al.* 1986, 1987; Maccagni *et al.* 1987, George, Warwick, and Bromage 1988; George, Warwick, and McHardy 1989; Barr, Giommi, and Maccagni 1988; Bregman *et al.* 1988; Treves *et al.* 1989). However, in many cases not all the observations of the same object have been presented or have appeared in different papers. Sometimes the analysis has been performed by different authors using different reduction systems, making an accurate and reliable comparison of the count rates a difficult, if not impossible, task. In addition, in a fair number of cases observations have never appeared in the literature.

In order to avoid difficulties in comparing count rates estimated by different authors using different reduction systems, we reanalyzed all the available data in a uniform way. Good agreement is found between our results and those already in the literature.

The objects in the sample are listed in Table 1, where column (1) gives the source name, column (2) the right ascension, column (3) the declination, column (4) the minimum[4] published radio flux density at 5 GHz (mostly measured with the VLA) with references given in column (5), column (6) the minimum reported optical magnitude with references in column (7), column (8) the redshift (when available), and column (9) the selection method, with "R" for radio-selected and "X" for X-ray or optically discovered BL Lacs.

A few BL Lacs detected in X-ray surveys were previously known at other frequencies (e.g., PKS 2155−304, ON 325, PKS 0548−322). In Table 1, however, these are listed as X-ray-selected. More than 200 observations of the 36 objects in the sample are available in the *EXOSAT* archive.

III. DATA ANALYSIS

The count rate in the channel multiplier array (CMA) detector (De Korte *et al.* 1981) was estimated in a square box, centered on the source centroid, and of a size such that the signal-to-noise ratio is expected to be maximum given the source strength, the background intensity, and the position of the source in the CMA field of view (FOV). The background level was estimated in a nearby source-free region of the image and rescaled to the position of the source to take into account detector nonuniformities (Giommi 1985). The background-subtracted counts were then corrected for vignetting effects, for the fraction of source photons expected to fall outside the box used, and for telemetry and instrumental dead times.

The count rates of all sources detected at large off axis angles (e.g., 1E 1415.6−2557, ON 235) were estimated taking into account the local CMA point spread function that was approximated using the method described in Giommi and Angelini (1987). Following this procedure, the systematic uncertainties in the count rates are $\approx 2\%$ near the center of the FOV and $\approx 10\%$ 40′ off-axis. In all cases systematic errors have been added quadratically to the statistical errors.

Since the CMA sensitivity remained constant throughout the mission (Giommi and Angelini 1987), all the count rates reported below are directly comparable.

The medium-energy (ME) experiment is described by Turner, Smith, and Zimmerman (1981). The ME experiment consists of a passively collimated proportional-counter array sensitive in the 0.7–50 keV region, though for weak sources there is effectively no signal above ~ 10 keV. One-half of the ME detector array was usually pointed at a blank region of the sky in order to monitor the particle background, the offset and on-source detectors being exchanged every 3 hr for optimum background subtraction. In those cases where array swaps were not performed, the background was estimated using the data from the slew onto or off the source (after careful examination of the light curves to avoid any sources which may have crossed the ME field of view during the slew).

The results of the data analysis are summarized in Table 2, where column (1) gives the source name, column (2) gives the observation date (year and day of the year), columns (3), (4), and (5) give the count rates in the thin Lexan, aluminum-parylene, and boron filters (when available) respectively; column (6) gives the count rate in the ME experiment. The count rates of Table 2 can be converted into fluxes using the conversion factors listed in Table 3, where column (1) gives the source name, column (2) gives the amount of interstellar absorbing material in the direction of the source (N_H, from Stark *et al.* 1990), columns (3), (4), (5), and (6) give the conversion factors between a count rate of 1 count s^{-1} and the flux in units of ergs cm^{-2} s^{-1} for the thin Lexan, aluminium-parylene, and boron filters and the ME detector, respectively.

Only two objects, MC 1057+100, and 4C 14.6, were not detected by the CMA. AO 0235+164 was observed nine times and, although not significantly detected in any single exposure, was detected when all the data were added together; 19 objects were also detected in the 0.7–8 keV band by the ME instrument. In three cases (1E 1415.6+2557, 2A 1218+304, and 3C 446), although a significant detection might have been achieved, confusion due to the presence of a second source in the 45′ FOV prevented a reliable measurement of the hard X-ray flux from the BL Lac. The remaining objects were undetected either because their flux was below the ME sensitivity limit or because a high particle background induced by enhanced solar activity or for both reasons. In the latter case no estimate of the 0.7–8 keV flux is given in Table 2.

IV. ME DETECTIONS DURING SLEWS

While *EXOSAT* was slewing from one target to the next, the ME experiment was kept operating and thus was able to

[4] Minimum optical and radio fluxes have been obtained from a bibliographic search from 1980 onward.

TABLE 1

THE SAMPLE

Source name (1)	R.A. (1950) h m s (2)	Dec. (1950) ° ′ ″ (3)	F_{5GHz} Jy (4)	Radio ref. (5)	m_V mag (6)	Optical ref. (7)	Redshift (8)	selection (9)
GC 0109+224	01 09 24	22 28 44	0.450	16	15.66	19		R
3C 66A	02 19 30	42 48 30	0.810	28	15.50	3	0.444	R
AO 0235+164	02 35 53	16 24 05	2.110	10	15.50	3	0.94	R
4C 47.08	03 00 10	47 04 34	1.920	10	17.21	3		R
1E 0317.0+1835	03 17 01	18 34 45	0.011	23	18.22	23	0.190	X
1H 0323+022	03 23 38	02 14 47	0.041	7	16.55	6	0.147	X
1H 0414+009	04 14 18	00 58 03	0.083	24	16.38	24		X
PKS 0521-365	05 21 13	-36 30 16	1.000	5	16.01	4	0.061	R
PKS 0548-322	05 48 50	-32 16 56	0.084	23	15.50	4	0.069	X
PKS 0735+178	07 35 14	17 49 09	2.010	13	16.76	4	0.424	R
PKS 0754+100	07 54 23	10 04 40	1.370	28	16.28	22		R
OJ 287	08 51 57	20 17 58	3.600	13	16.58	21	0.306	R
MC 1057+100	10 57 44	10 05 42	0.110	27	17.76	3		R
MKN 421	11 01 41	38 28 43	0.530	25	13.89	18	0.031	X
MKN 180	11 33 30	70 25 00	0.251	12	14.95	15	0.046	X
B2 1147+245	11 47 44	24 34 35	0.740	17	16.00	11		R
1E 1207.9+3945	12 07 55	39 45 49	0.006	23	19.48	23	0.59	X
ON 325	12 15 21	30 23 40	0.380	25	15.50	29		R
2A 1218+304	12 18 52	30 27 14	0.042	23	16.50	4	0.13	X
1E 1235.4+6315	12 35 26	63 15 12	0.007	23	20.07	23	0.297	X
B2 1308+326	13 08 08	32 36 40	1.900	14	19.00	3	0.996	R
1E 1402.3+0416	14 02 20	04 16 22	0.021	23	17.55	23		X
1E 1415.6+2557	14 15 41	25 57 15	0.054	9	16.00	9	0.237	X
OQ 530	14 18 06	54 36 57	1.760	14	16.18	22		R
1H 1427+42	14 26 36	42 53 46	0.034*	20	16.42	20	0.129	X
AP Librae	15 14 45	-24 11 22	1.840	14	15.80	2	0.049	R
4C 14.60	15 38 31	14 57 25	1.140	27	17.30	4		R
MKN 501	16 52 12	39 50 26	1.200	15	14.17	18	0.034	X
4U 1722+11	17 22 44	11 54 52	0.079	8	16.60	8		X
I ZW 186	17 27 04	50 15 31	0.150	27	16.24	1	0.055	X
1803+78	18 03 39	78 27 54	2.100	17	17.00	3		R
3C 371	18 07 18	69 48 59	1.450	17	14.81	4	0.051	R
PKS 2005-489	20 05 47	-48 58 43	1.190	26	15.30	3		X
PKS 2155-304	21 55 58	-30 27 52	0.341	23	14.80	4	0.117	X
BL Lac	22 00 39	42 02 08	2.390	10	15.74	22	0.07	R
3C 446	22 23 11	-05 12 17	2.400	25	17.90	3	1.404	R

* 1.4 GHz.

REFERENCES—(1) Bregman *et al.* 1982; (2) Brindle *et al.* 1986; (3) Burbidge and Hewitt 1987; (4) Cruz-Gonzales and Huchra 1984; (5) Danziger *et al.* 1979; (6) Doxey *et al.* 1983; (7) Feigelson *et al.* 1986; (8) Griffiths *et al.* 1989; (9) Halpern *et al.* 1986; (10) Jones *et al.* 1981; (11) Kinman 1976; (12) Kuhr *et al.* 1981; (13) Landau *et al.* 1983; (14) Landau *et al.* 1986; (15) Mufson *et al.* 1984; (16) Owen, Spangler, and Cotton 1980; (17) Perley 1982; (18) Pica *et al.* 1980; (19) Puschell and Stein 1980; (20) Remillard *et al.* 1987; (21) Sitko and Junkkarinen 1985; (22) Smith *et al.* 1987; (23) Stocke *et al.* 1985; (24) Ulmer *et al.* 1983; (25) Ulvestad, Johnston, and Weiler 1983; (26) Wall *et al.* 1975; (27) Weiler and Johnston 1980; (28) Worrall *et al.* 1984*a*; (29) Worrall *et al.* 1984*b*.

observe cosmic X-ray sources that passed through its field of view. In this way the entire sky was covered, providing a survey with a lower sensitivity limit of a few ME counts s^{-1}, as described in detail by Pollock *et al.* (1990). Pointlike sources were detected as local maxima of the characteristic triangular-shaped collimator response in channels 6–24 above a background estimated simultaneously from channels 40–60, which are almost invariably filled with background events. The time at which a source passed through the center of the collimator can be estimated with an accuracy of a fraction of a second, leading to an error box of dimension a few arcminutes along the slew direction and, in turn, leaving no doubt of the identification of many of the sources detected.

Three of these sources were BL Lac objects in our sample. Their intensities are listed in Table 2.

Because the sensitivity of the typically 2 minute observations of the ME slew survey was comparatively low, only a few of the brightest sources, when in a sufficiently high state, were detected.

V. ENERGY DISTRIBUTION AND FLUX CORRELATIONS

An illustration of the (nonsimultaneous) radio through X-ray energy distribution of all the detected objects in the sample is given in Figure 1, where the two-point spectral indices between radio and optical band (α_{ro}) and between optical and soft X-ray energy band (α_{ox}) are plotted. Here $\alpha_{ro} = \log(S_{5\,\mathrm{GHz}}/S_{2500\,\mathrm{Å}})/5.38$ and $\alpha_{ox} = -\log(S_{2\,\mathrm{keV}}/S_{2500\,\mathrm{Å}})/2.605$, where $S_{5\,\mathrm{GHz}}$, $S_{2500\,\mathrm{Å}}$, and $S_{2\,\mathrm{keV}}$ are the monochromatic fluxes at 5 GHz, 2500 Å, and 2 keV, respectively. When more than one observation of an object was available, α_{ox} and α_{ro} were calculated using the minimum reported flux. Open circles correspond to *EXOSAT* observations of radio-selected BL Lacs, and asterisks to X-ray–selected sources. Filled circles are a sample of 30 BL Lacs discovered in the *Einstein* EMSS (Maccacaro *et al.* 1989). The dashed line represents the correlation found by Ledden and O'Dell (1985) in a sample of blazars (a subclass of AGNs including BL Lacs, highly polarized QSOs, and optically violent variable QSOs) observed

TABLE 2

Count Rates

source name (1)	date (2)	thin lexan (10^{-3}cts/s) (3)	al/p (10^{-3}cts/s) (4)	boron (10^{-3}cts/s) (5)	ME (ch 4-34) (cts/s) (6)
GC 0109+224	84-224	1.6 ± 0.5			
3C 66A	86-006	3.8 ± 0.7			0.31 ± 0.02
	86-015	< 2.8			0.40 ± 0.07
	86-032	2.5 ± 0.5			0.46 ± 0.03
AO 0235+164	83-341	< 2.7	< 12.		
	83-343	< 3.6			
	83-345	< 2.8			
	83-348	< 4.1			
	84-214	< 2.3			
	85-025	< 2.0			
	86-006	< 1.7			
	86-015	< 2.5			
	86-032	< 6.4			
	Σ^{a}	0.7 ± 0.2			
4C 47.08	84-046	2.1 ± 0.8			
1E 0317.0+1835	85-013	8.9 ± 1.8			0.77 ± 0.09
	85-039	7.9 ± 1.3			0.62 ± 0.04
1H 0323+022	84-265	32.3 ± 3.7	27.6 ± 3.5	7.3 ± 1.4	1.07 ± 0.95
	84-267	27.5 ± 1.8			0.82 ± 0.04
	85-023	9.3 ± 1.1			< 0.42
	85-025	7.9 ± 0.8			< 0.15
	86-004	7.4 ± 0.8			< 0.18
	86-007	6.7 ± 0.8			< 0.12
1H 0414+009	84-253	32.3 ± 4.3	22.3 ± 3.0	16.9 ± 3.1	2.03 ± 0.05
	84-258	36.9 ± 3.3	26.4 ± 2.4		2.38 ± 0.05
	84-266	38.4 ± 4.5	21.0 ± 2.1		1.40 ± 0.05
	84-274	38.3 ± 3.9	25.3 ± 3.0		1.18 ± 0.06
PKS 0521-365	83-306	11.3 ± 1.8	10.8 ± 1.7		0.81 ± 0.04
	83-334	17.3 ± 2.4	8.3 ± 2.2		0.89 ± 0.07
PKS 0548-322	83-306	115. ± 7.	61.9 ± 6.4	11.5 ± 2.2	2.55 ± 0.05
	83-334	115. ± 14.	59.5 ± 7.1	19.5 ± 3.0	2.56 ± 0.07
	86-066	92.0 ± 1.0			1.77 ± 0.02
PKS 0735+178	83-316	2.2 ± 0.5			(b)
	83-317	1.5 ± 0.5			(b)
	83-318	3.8 ± 0.7			(b)
PKS 0754+100	84-044	7.0 ± 0.9	2.7 ± 0.7		0.38 ± 0.06
OJ 287	83-281	35.5 ± 3.3			
	83-341	23.5 ± 3.2	8.5 ± 1.8	< 3.1	
	84-038	38.9 ± 2.9			
	84-039	49.4 ± 3.0	20.5 ± 2.8	3.7 ± 1.3	
	84-040	41.3 ± 5.7		2.8 ± 0.8	
	84-112	15.0 ± 6.4		3.9 ± 1.2	
	84-344	10.0 ± 1.7			
	84-345	9.5 ± 0.7			
	85-341	7.8 ± 0.6			
	85-342	8.9 ± 0.7			
	85-346	9.1 ± 0.6			
MC 1057+100	84-150	< 2.4			
MKN 421	84-032	499. ± 14.	182. ± 5.		1.14 ± 0.06
	84-033	328. ± 12.	113. ± 8.	22.8 ± 4.2	0.58 ± 0.15
	84-035	421. ± 18.	156. ± 7.	31.4 ± 3.5	0.99 ± 0.12
	84-037	483. ± 13.	170. ± 8.	32.9 ± 4.2	1.21 ± 0.06
	84-326				6.2 ± 1.4 (c)
	84-337	852. ± 23.	363. ± 11.	101. ± 6.	10.16 ± 0.06
	84-338	1093. ± 21.	470. ± 9.	116. ± 4.	12.74 ± 0.05
	84-340	1082. ± 27.	498. ± 13.	126. ± 6.	12.36 ± 0.12
	85-004	474. ± 23.	174. ± 11.	29.2 ± 3.5	1.53 ± 0.06
	85-023				11.6 ± 2.3 (c)
	85-112	548. ± 10.	235. ± 7.	42.9 ± 3.9	2.79 ± 0.04
	85-118	426. ± 9.	177. ± 6.	35.8 ± 3.2	2.73 ± 0.04
	85-126	425. ± 9.	173. ± 5.	28.3 ± 2.5	1.15 ± 0.04
	85-131	488. ± 10.	189. ± 6.	34.1 ± 3.2	2.80 ± 0.04
	85-132	461. ± 12.			1.67 ± 0.08
	85-141	382. ± 9.	154. ± 6.	31.4 ± 3.0	1.65 ± 0.06

TABLE 2—*Continued*

source name (1)	date (2)	thin lexan (10^{-3}cts/s) (3)	al/p (10^{-3}cts/s) (4)	boron (10^{-3}cts/s) (5)	ME (ch 4-34) (cts/s) (6)
MKN 180	84-308	73.9 ± 7.6	30.4 ± 4.6		0.15 ± 0.05
	84-317	83.7 ± 10.3	42.2 ± 9.5		< 0.60
	84-325	78.7 ± 5.5			< 1.38
	84-333	96.7 ± 6.0	45.3 ± 4.4	7.72 ± 1.5	0.39 ± 0.03
	85-093	173. ± 12.	71.4 ± 5.4	18.3 ± 3.0	1.08 ± 0.04
B2 1147+245	84-016	< 5.0			
	84-017	3.6 ± 0.5			
	84-018	3.2 ± 0.6			
1E 1207.9+3945	83-192	8.5 ± 1.7			(d)
	83-311	5.5 ± 1.7	3.2 ± 0.9		(d)
	83-315	7.1 ± 2.2	5.7 ± 1.7		(d)
	83-319	6.0 ± 1.8			(d)
	83-323	< 8.2			(d)
	83-351	6.3 ± 0.7			(d)
	84-098	8.4 ± 1.7	4.9 ± 1.1		(d)
	84-109	9.4 ± 1.8	3.4 ± 1.1		(d)
	84-154	< 14.	< 5.8		(d)
	84-351	7.4 ± 2.4			(d)
	84-354	6.3 ± 1.7			(d)
	84-357		4.5 ± 1.4		(d)
	85-002	5.9 ± 1.8			(d)
	85-027	6.4 ± 0.9			(d)
	85-111	7.3 ± 1.3	5.0 ± 1.3		(d)
	85-118	8.6 ± 1.3	5.3 ± 1.2		(d)
	85-128	8.3 ± 1.5	6.0 ± 1.2		(d)
	85-135	7.6 ± 1.1	3.6 ± 1.0		(d)
	85-136	7.2 ± 1.8			(d)
	85-143	7.6 ± 2.0			(d)
	85-150	9.1 ± 1.4			(d)
	86-062	8.9 ± 1.9			(d)
ON 325	83-353	79.8 ± 6.2	35.3 ± 3.1	2.9 ± 0.5	(e)
	84-031	94.5 ± 14.5	35.9 ± 8.5		(e)
	84-033	< 12.			(e)
	84-035	50.7 ± 15.8	< 42.		(e)
	84-037	39.9 ± 9.1	26.4 ± 6.9		(e)
	84-356	45.2 ± 10.0			(e)
	85-005	56.3 ± 10.8	< 50.		(e)
	85-020	< 68.			(e)
	85-029	50.6 ± 10.5	< 51.		(e)
	85-131	52.2 ± 4.8	24.2 ± 6.8		(e)
	85-131	51.3 ± 7.8	23.2 ± 2.4		(e)
	85-363	55.5 ± 6.6			(e)
	85-365	21.1 ± 3.3			(e)
	86-014	18.0 ± 3.9			(e)
2A 1218+304	83-353	178. ± 32.	104. ± 19.		(f)
	84-031	216. ± 8.	101. ± 7.	15.6 ± 2.8	(f)
	84-033	243. ± 16.	128. ± 16.	24.8 ± 3.1	(f)
	84-035	251. ± 15.	140. ± 7.	27.9 ± 3.3	(f)
	84-037	280. ± 10.	141. ± 7.	27.0 ± 3.1	(f)
	84-156	108. ± 14.	< 98.		(f)
	84-356	208. ± 8..	102. ± 5.	13.6 ± 2.7	(f)
	85-005	203. ± 9.	106. ± 8.	24.7 ± 3.1	(f)
	85-020	206. ± 11.	116. ± 7.	18.0 ± 2.5	(f)
	85-029	182. ± 7.	101. ± 6.	11.0 ± 3.1	(f)
	85-131	178. ± 19.	83.6 ± 13.0		(f)
	85-131	170. ± 28.	91.0 ± 11.1		(f)
	86-014	137. ± 3.	68.4 ± 5.2	15.1 ± 1.9	(f)
1E 1235.4+6315	85-079	2.8 ± 0.6			
B2 1308+326	84-059	8.4 ± 1.6	< 7.1		< 4.2
	84-066	6.6 ± 1.3	3.3 ± 0.9		< 0.33
	84-068	5.4 ± 1.3	< 3.0		
	84-069	4.0 ± 0.9			< 0.32
	85-121	6.3 ± 1.1			< 0.46
	85-132	6.7 ± 1.1	1.7 ± 0.6		0.20 ± 0.02
	85-149	7.3 ± 1.1			0.14 ± 0.03
	85-164	5.4 ± 1.0			0.17 ± 0.03

TABLE 2—*Continued*

source name (1)	date (2)	thin lexan (10^{-3}cts/s) (3)	al/p (10^{-3}cts/s) (4)	boron (10^{-3}cts/s) (5)	ME (ch 4-34) (cts/s) (6)
1E 1402.3+0416	85-031	27.8 ± 2.1	11.0 ± 1.0		0.24 ± 0.04
	85-031	14.0 ± 2.5	6.5 ± 1.5		0.20 ± 0.06
	85-037	12.0 ± 2.5			
	85-187	13.4 ± 1.4			0.20 ± 0.04
1E 1415.6+2557	84-032	83.3 ± 14.6			(g)
	84-062	50.1 ± 12.2			(g)
	84-141	66.6 ± 8.8			(g)
	84-193	72.5 ± 8.2			(g)
	85-014	64.9 ± 11.4			(g)
	85-062	67.8 ± 12.1			(g)
	85-159	64.6 ± 10.6	22.2 ± 5.2		(g)
	85-173	76.1 ± 11.6			(g)
	85-186	57.2 ± 9.9			(g)
	85-195	57.4 ± 11.0			(g)
	86-019	56.3 ± 6.4			(g)
	86-062	49.5 ± 5.6			(g)
	86-063	60.3 ± 1.7			0.62 ± 0.04 (h)
OQ 530	84-139	7.5 ± 1.5	3.7 ± 1.6		
	84-140	6.8 ± 0.9		< 3.0	
	84-141	5.9 ± 0.9			
1H 1427+42	85-012	327. ± 8.			3.36 ± 0.05
	85-055	287. ± 12.	116. ± 11.	29.1 ± 3.2	2.56 ± 0.06
AP Lib	83-229	2.6 ± 0.4			
4C 14.60	84-054	< 2.2			
MKN 501	84-032	431. ± 13.	193. ± 10.	47.0 ± 4.2	3.80 ± 0.14
	84-034				4.2 ± 1.2 (c)
	84-034	421. ± 12.	201. ± 11.	50.2 ± 7.1	4.00 ± 0.06
	84-036	425. ± 11.	190. ± 7.	41.9 ± 3.8	3.30 ± 0.12
	84-086	370. ± 20.			0.74 ± 0.06
	84-183	401. ± 17.	165. ± 7.	37.4 ± 3.9	2.31 ± 0.07
	84-191	364. ± 12.	158. ± 9.	27.3 ± 4.7	2.70 ± 0.11
	84-201	353. ± 14.	149. ± 8.	25.4 ± 3.4	2.54 ± 0.05
	84-207	380. ± 19.	182. ± 12.	37.9 ± 3.4	1.52 ± 0.08
	84-209	362. ± 17.	167. ± 8.	37.8 ± 3.4	2.84 ± 0.08
	85-099	363. ± 13.	165. ± 6.	33.9 ± 3.0	2.03 ± 0.05
	85-237				5.4 ± 1.5 (c)
	86-074	380. ± 3.			3.95 ± 0.10
4U 1722+11	85-246	25.1 ± 2.8	17.3 ± 2.4	4.0 ± 1.4	0.58 ± 0.02
I ZW 186	84-063	61.5 ± 3.9	40.5 ± 3.3	8.4 ± 0.8	0.66 ± 0.11
	84-181	80.2 ± 4.2	43.0 ± 4.4	8.9 ± 1.4	0.70 ± 0.04
1803+78	83-251	2.84 ± 0.5			
	83-266	2.36 ± 0.5			
	83-281	2.2 ± 0.6			
	83-296	2.0 ± 0.4			
3C 371	84-255	45.6 ± 1.6	25.1 ± 2.7	2.3 ± 0.8	0.35 ± 0.04
	84-273	22.0 ± 1.4	11.8 ± 1.8		0.23 ± 0.04
PKS 2005-489	84-254	436. ± 18.	250. ± 11.	44.8 ± 2.7	2.82 ± 0.04
	84-287	596. ± 24.	320. ± 15.	60.3 ± 5.0	6.30 ± 0.06
	85-144	51.6 ± 3.8	29.3 ± 2.8	4.0 ± 1.2	0.16 ± 0.04
	85-276	61.0 ± 4.2	36.1 ± 2.5		0.30 ± 0.08
	85-289	150. ± 8.	82.9 ± 4.8	10.0 ± 1.6	0.55 ± 0.06
PKS 2155-304	83-304	828. ± 13.	250. ± 7.	35.6 ± 2.8	1.99 ± 0.03
	83-304	690. ± 15.	214. ± 6.	27.4 ± 2.3	
	83-333	1340. ± 38.	465. ± 23.	64.1 ± 4.3	4.22 ± 0.09
	84-311	1970. ± 36.	681. ± 18.	122. ± 5.	6.25 ± 0.10
	84-311	2259. ± 49.			10.19 ± 0.07
	84-312	2058. ± 42.	779. ± 23.	155. ± 5.	7.63 ± 0.06
	84-312	3169. ± 50.			17.62 ± 0.17
	84-316	2370. ± 73.	891. ± 43.	109. ± 5.	7.80 ± 0.10
	84-316	2264. ± 39.			7.30 ± 0.10
	85-145				11.2 ± 1.8 (c)
	85-297	3734. ± 10.			16.04 ± 0.04
	85-305	1786. ± 31.	636. ± 15.		4.70 ± 0.11
	85-306	1850. ± 7.			4.89 ± 0.03
	85-316	1357. ± 6.			2.62 ± 0.02

TABLE 2—*Continued*

source name (1)	date (2)	thin lexan (10^{-3}cts/s) (3)	al/p (10^{-3}cts/s) (4)	boron (10^{-3}cts/s) (5)	ME (ch 4-34) (cts/s) (6)
BL Lac	83-341	4.3 ± 0.6			
3C 446	83-327	7.9 ± 2.8			(i)
	83-336	11.3 ± 2.0	8.2 ± 1.8		(i)
	83-340	8.5 ± 1.5	3.7 ± 1.1		(i)
	83-343	6.8 ± 1.5	6.3 ± 1.5		(i)
	83-345	5.2 ± 1.2			(i)
	84-152	2.8 ± 0.7			(i)
	84-299	3.0 ± 0.8			(i)
	85-148	< 4.5			(i)
	85-157	< 4.7			(i)
	85-164	1.7 ± 0.6			(i)
	85-171	2.6 ± 0.8			(i)
	85-180	3.1 ± 0.9			(i)
	85-184	< 5.0			(i)

[a] Sum of all exposures.
[b] Confused with a serendipitous AGN.
[c] Source detected during slew (the count rate is calculated in channels 3–24).
[d] Confused with NGC 4151.
[e] Confused with Mrk 766 and 2A 1218+304.
[f] Confused with Mrk 766 and ON 325.
[g] Source at the edge of the CMA image and only marginally included in ME FOV, which was centered on the Seyfert galaxy NGC 5548.
[h] On this occasion pointing was offset to avoid confusion with NGC 5548.
[i] Confused with PHL 5200.

with the *Einstein Observatory*. The distribution of the points in Figure 1 is clearly bimodal, with most of the radio-selected objects clustered near the dashed line. All the X-ray and optically selected BL Lac objects are confined instead to a region of the plane defined by $0.3 < \alpha_{ro} < 0.6$ and $\alpha_{ox} < 1.2$ (i.e., characterized by strong X-ray emission but with moderate radio emission relative to the optical). This behavior has been noted by other authors in samples of BL Lacs observed with the *Einstein* satellite (e.g., Stocke *et al.* 1985; Stocke *et al.* 1988; Ledden and O'Dell 1985). A detailed statistical analysis of *Einstein* data of radio-loud QSOs (Worrall *et al.* 1987) has shown that these sources are characterized by an energy distribution which is very similar to that of blazars. Although the statistical analysis was based on a different parameterization, the best-fit values to the relation between radio, optical, and X-ray luminosities, for the subsample of QSOs with flat radio spectra, are essentially equivalent to those obtained by Ledden and O'Dell (1985).

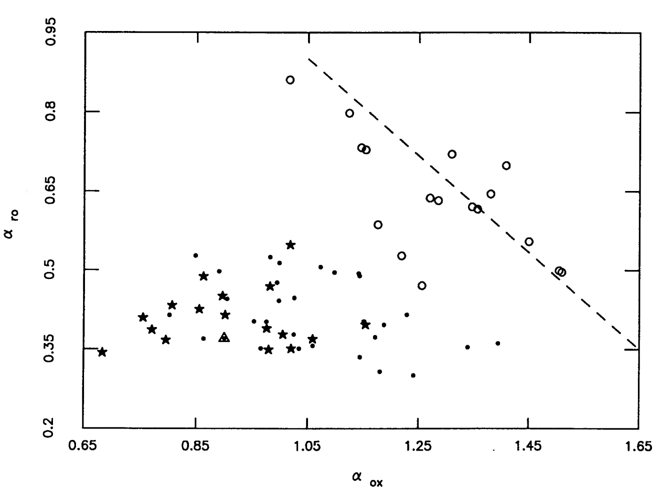

FIG. 1.—The α_{ox}-α_{ro} diagram of BL Lac objects. *EXOSAT* X–BL Lacs are represented by asterisks, *EXOSAT* Q–BL Lacs by open circles, and *Einstein* EMSS BL Lacs by small circles. The Crab pulsar is shown as a triangle. The dashed line represents a correlation found by Ledden and O'Dell (1985) in a sample of radio-selected blazars.

Throughout this paper we will refer to the sources that lie near the dashed line as the quasar-like BL Lacs (or Q–BL Lacs), and to the remaining objects as the X-ray strong BL Lacs (or X–BL Lacs).

In Figures 2*a* and 2*b* the minimum soft X-ray flux of each object measured by *EXOSAT* is plotted against the radio flux density at 5 GHz for the subsample of the X–BL Lacs and Q–BL Lacs, respectively. A correlation between the fluxes in the two bands is present in the subsample of the X–BL Lacs. The probability that such a correlation arises by chance from a sample randomly extracted from an uncorrelated parent population is $P = 2 \times 10^{-4}$. No correlation is present in the subsample of Q–BL Lacs ($P = 0.74$). The difference between the two is even more striking in Figures 3*a* and 3*b*, where the radio flux density is plotted against the apparent visual magnitude. A tight correlation between radio and optical fluxes is apparent in the X–BL Lac sample. The linear best fit is $\log F_R = -0.38 \times m_V + 8.12$, and the significance is $P = 4 \times 10^{-7}$. This dependence is equivalent to the narrow distribution of α_{ro} that has been noted in other samples of X-ray-selected BL Lacs (e.g., Stocke *et al.* 1988). F_R and m_V appear to be uncorrelated in the sample of Q–BL Lacs, where both the Spearman's rank and Kendall's τ correlation tests give a chance probability of ≈ 0.3.

VI. TIME VARIABILITY

a) Medium and Long-Term Flux Variability

Of the 36 objects in our sample, 26 were detected more than once in the CMA and 15 in the ME. In order to study their long-term X-ray variability, we have performed a standard χ^2 analysis to test constancy in each source. We discuss below the objects with chance χ^2 probabilities less than 10^{-3}. Fifteen out of 26 CMA objects (58%) and 11 out of the 15 ME objects

TABLE 3

CONVERSION FACTORS BETWEEN COUNT RATE AND FLUX[a]

Source name (1)	N_H cm^{-2} units of 10^{20} (2)	thin lexan $erg\ cm^{-2}\ ct^{-1}$ 0.05-2.0keV units of 10^{-10} (3)	al/par $erg\ cm^{-2}\ ct^{-1}$ 0.05-2.0keV units of 10^{-10} (4)	boron $erg\ cm^{-2}\ ct^{-1}$ 0.05-2.0keV units of 10^{-10} (5)	ME $erg\ cm^{-2}\ ct^{-1}$ 2-6 keV units of 10^{-12} (6)
GC 0109+224	4.6	4.0	6.0	18.7	7.9
3C 66A	7.5	5.0	6.9	17.6	7.9
AO 0235+164	9.1	5.4	7.3	17.2	7.9
4C 47.08	19.	7.2	9.4	16.2	7.9
1E 0317.0+1835	9.8	5.6	7.5	17.0	7.9
1H 0323+022	8.4	5.3	7.1	17.3	7.9
1H 0414+009	8.3	5.2	7.1	17.3	7.9
PKS 0521-365	3.5	3.5	5.6	19.2	7.9
PKS 0548-322	2.3	2.8	5.1	19.5	7.9
PKS 0735+178	4.7	4.1	6.1	18.6	7.9
PKS 0754+100	2.7	3.0	5.3	19.5	7.9
OJ 287	3.0	3.2	5.4	19.4	7.9
MC 1057+100	2.4	2.8	5.2	19.5	7.9
MKN 421	1.8	2.4	4.9	19.2	7.9
MKN 180	1.4	2.1	4.6	18.4	7.9
B2 1147+245	2.0	2.6	5.0	19.4	7.9
1E 1207.9+3945	2.1	2.6	5.1	19.5	7.9
ON 325	1.6	2.2	4.7	18.8	7.9
2A 1218+304	1.7	2.3	4.8	19.0	7.9
1E 1235.4+6315	1.7	2.3	4.8	19.0	7.9
B2 1308+326	1.1	1.8	4.4	17.4	7.9
1E 1402.3+0416	2.2	2.7	5.1	19.5	7.9
1E 1415.6+2557	1.6	2.2	4.7	18.8	7.9
OQ 530	1.3	2.0	4.6	18.1	7.9
1H 1427+42	1.4	2.1	4.6	18.4	7.9
AP Librae	8.8	5.4	7.2	17.2	7.9
4C 14.60	3.2	3.3	5.5	19.3	7.9
MKN 501	1.7	2.3	4.8	19.0	7.9
4U 1722+11	8.6	5.3	7.2	17.3	7.9
I ZW 186	2.7	3.0	5.3	19.5	7.9
1803+78	4.0	3.8	5.8	19.0	7.9
3C 371	4.9	4.2	6.1	18.6	7.9
PKS 2005-489	4.6	4.0	6.0	18.7	7.9
PKS 2155-304	1.8	2.4	4.6	19.2	7.9
BL Lac	19.	7.2	9.4	16.2	7.9
3C 446	5.5	4.4	6.3	18.3	7.9

[a] Assuming a power-law spectrum with energy index $\alpha = 1.0$ and N_H equal to the value given in column (2). To convert from ergs cm^{-2} s^{-1} in the 0.05–2.0 keV band or in the 2–6 keV band to μJy at 1 keV, multiply the values given in the table by 1.1×10^{11} or by 3.8×10^{11}, respectively.

(73%) showed significant variability according to this test. With the exception of PKS 0521−365 and 1E 0317.0+1835, which were observed only twice, negative results were confined to the weaker sources; whenever a source was sufficiently bright to allow the detection of variability of $\approx$20%, significant variability was seen. The results are summarized in Table 4, where column (1) gives the source name; for the LE experiment, column (2) gives the number of observations, column (3) the χ^2 value, column (4) the number of degrees of freedom, and column (5) the corresponding probability; columns (6), (7), and (8) are the same for the ME experiment.

The X-ray light curves of the objects that were observed at least 4 times or that showed significant luminosity variability are shown in Figures 4*a*–4*h* and Figures 5*a*–5*h*. Whenever a source was detected by the ME instrument, and not confused, both the count rate measured in the thin Lexan filter and that in the ME instrument are plotted against observation time. The scales on the *y*-axes are logarithmic, so that variability of the same amplitude in both instruments correspond to equal vertical separation between the points (see Figs. 5*a*–5*h*). Each point is the average count rate during the whole observation unless significant variability within a single exposure was detected, in which case the observation was divided into two or more parts and the different count rates appear on the light curve as separate measurements.

Visual inspection of the light curves of the sources for which both LE and ME data are available (Figs. 5*a*–5*h*) shows that in several cases (e.g., 1H 0323+022, 1H 0414+009, Mrk 421, Mrk 180, Mrk 501) flux variations in the ME experiment (0.7–8 keV) are more pronounced than those in the CMA. A comparison between *Einstein* imaging proportional counter (IPC) and monitor proportional counter (MPC) data also indicated a similar difference in variability between soft and hard X-rays in some BL Lac objects (Schwartz and Madejski 1986). This difference in the variability properties in the two energy bands implies changes in the sources' spectral shape and is better studied by analyzing the hardness ratio as a function of source intensity.

b) Rapid Variability

A systematic search for rapid variability was performed on all LE and ME observations which produced a significant detection. Unfortunately, the frequent filter changes made during many LE observations was a major complication for

TABLE 4

SUMMARY OF LONG-TERM VARIBILITY ANALYSIS

Source name	number of observations	thin lexan χ^2	thin lexan d.o.f	thin lexan P	ME χ^2	ME d.o.f.	ME P
3C 66A	3	2.28	1	0.13	4.73	2	9.4×10^{-2}
1E 0317.0+1835	2	0.20	1	0.65	8.02	1	3.6×10^{-4}
1H 0323+022	6	159.4	5	0.00	19.6	1	7.3×10^{-7}
1H 0414+009	4	1.36	3	0.72	426.0	3	0.00
PKS 0521-365	2	4.00	1	4.6×10^{-2}	0.03	1	0.99
PKS 0548-322	3	13.2	2	1.4×10^{-3}	245.5	2	0.00
PKS 0735+178	3	6.51	2	3.9×10^{-2}			
OJ 287	11	394.3	10	0.00			
MKN 421	14	2040	13	0.00	7.4×10^4	12	0.00
MKN 180	5	57.7	4	8.9×10^{-12}		2	0.00
B2 1147+245	3	0.06	1	0.80			
1E 1207.9+3945	22	11.65	18	0.86			
ON 325	14	138.7	11	0.00			
2A 1218+304	13	425.4	12	0.00			
B2 1308+326	8	9.37	7	0.23	2.88	2	0.24
1E 1402.3+0416	4	38.1	3	2.7×10^{-8}			
1E 1415.6+2557	13	12.8	12	0.39			
OQ 530	3	0.93	2	0.63			
1H 1427+42	2	7.46	1	4.9×10^{-4}	104.9	1	0.00
MKN 501	11	52.0	10	1.1×10^{-7}	4479	10	0.00
I ZW 186	2	10.7	1	1.1×10^{-3}	0.37	1	0.96
1803+78	3	0.34	2	0.84			
3C 371	2	123.8	1	0.00	10.9	1	7.4×10^{-5}
PKS 2005-489	5	994.0	4	0.00	1.1×10^4	4	0.00
PKS 2155-304	13	5.5×10^4	12	0.00	1.6×10^5	12	0.00
3C 446	13	46.6	9	4.7×10^{-7}			

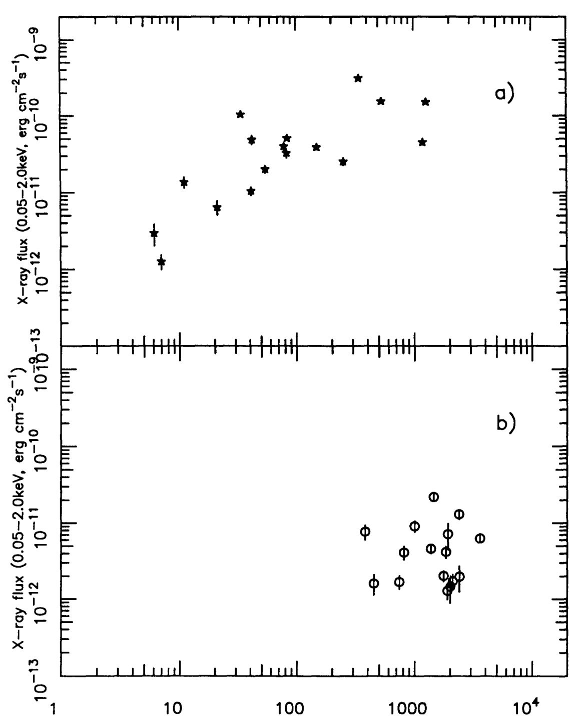

FIG. 2.—Minimum observed X-ray flux plotted against radio flux density for (*a*) X–BL Lacs and (*b*) Q–BL Lacs.

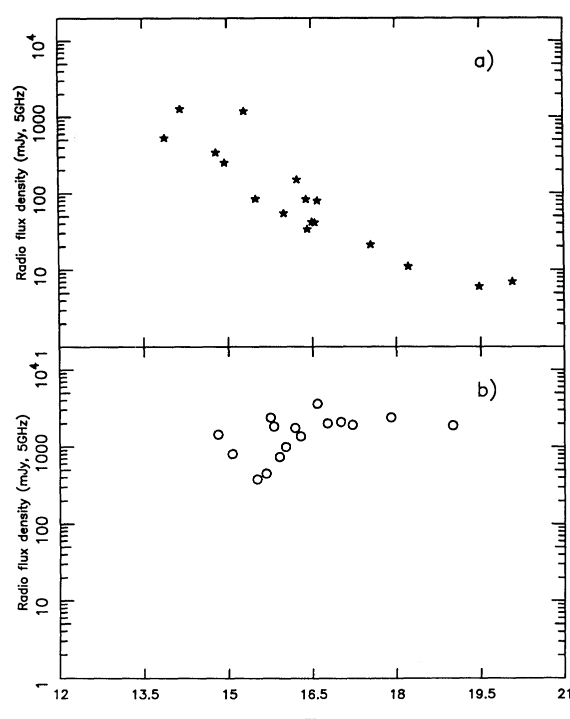

FIG. 3.—Radio flux density plotted against optical apparent magnitude for (*a*) X–BL Lacs and (*b*) Q–BL Lacs.

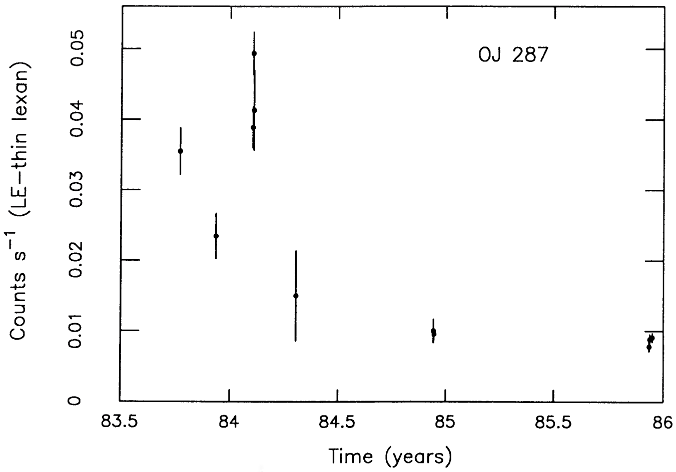

FIG. 4*a*

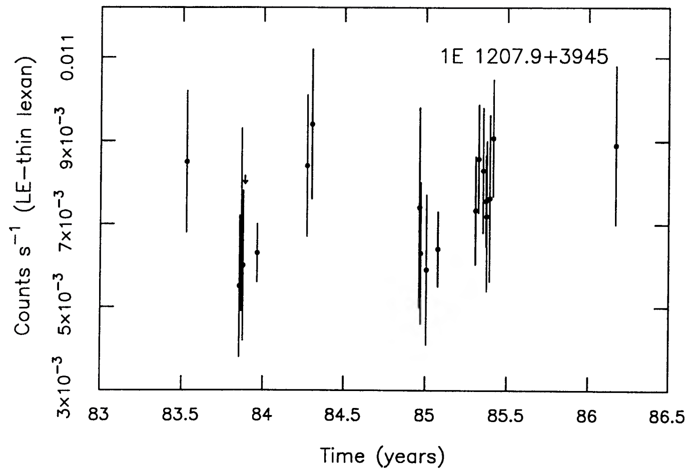

FIG. 4*b*

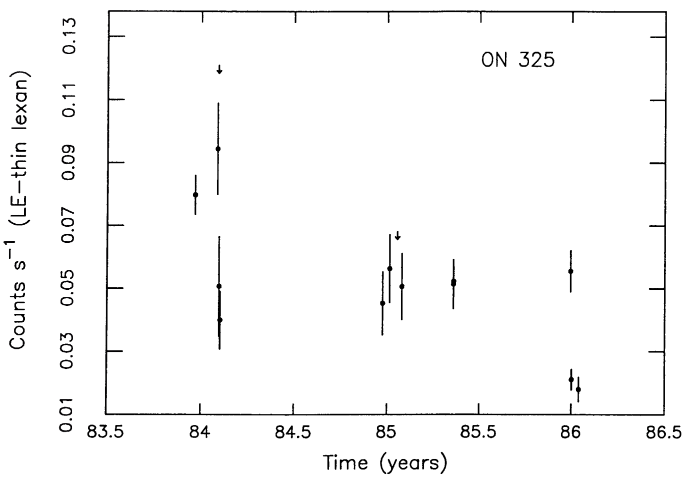

FIG. 4*c*

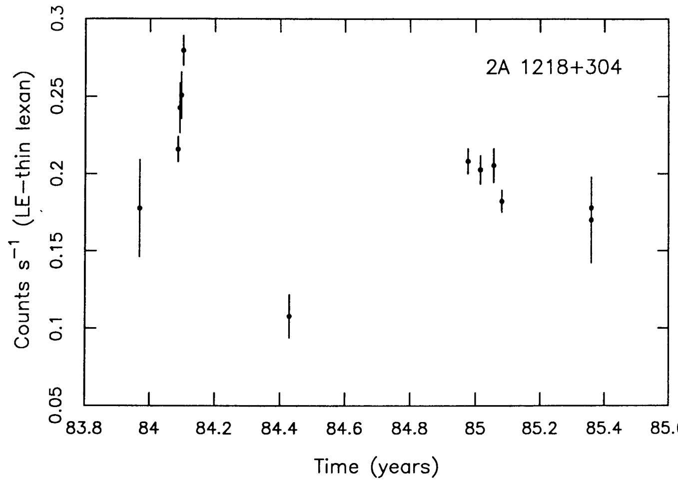

FIG. 4*d*

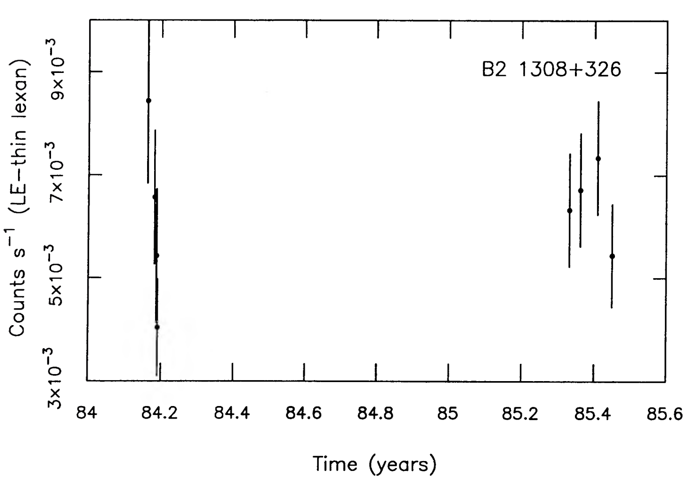

FIG. 4*e*

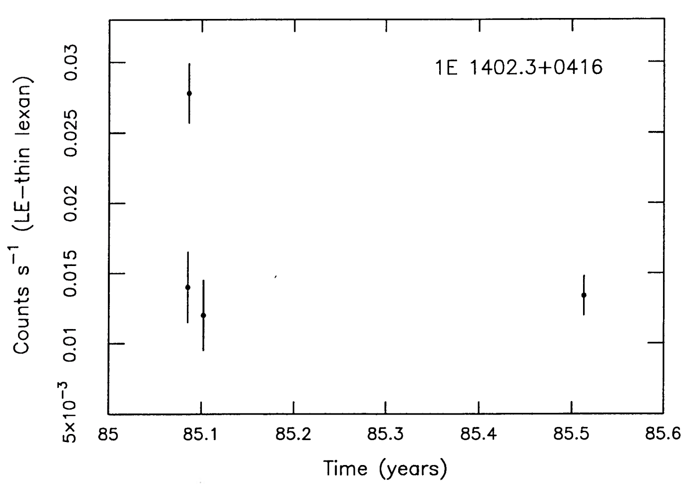

FIG. 4*f*

FIG. 4.—Long-term soft X-ray light curves of all BL Lacs in the sample which were detected at least 4 times by the CMA but not by the ME detectors, or showed significant variability. (*a*) OJ 287, (*b*) 1E 1207.9 + 3945, (*c*) ON 325, (*d*) 2A 1218 + 304, (*e*) B2 1308 + 326, (*f*) 1E 1402.3 + 0416, (*g*) 1E 1415.6 + 2557, (*h*) 3C 446.

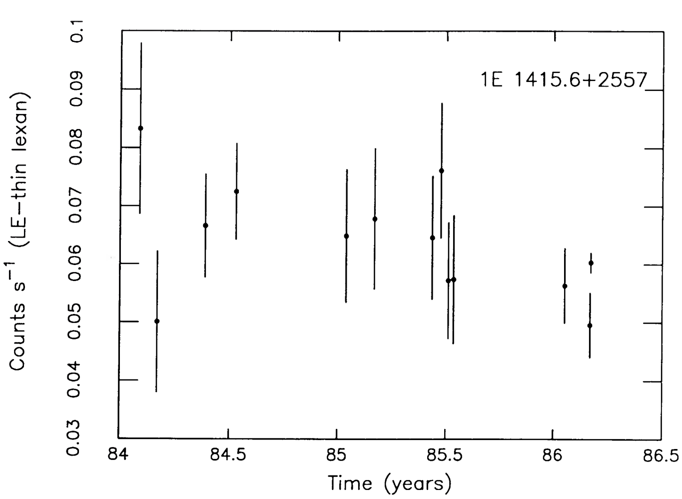

FIG. 4*g*

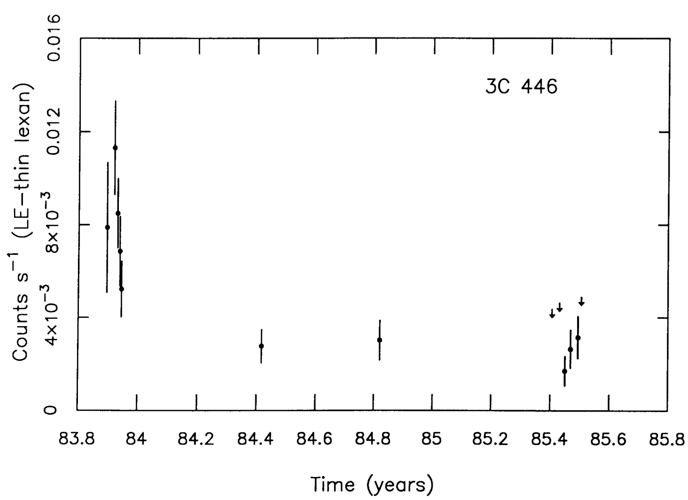

FIG. 4*h*

FIG. 4—*Continued*

the analysis of the CMA data. Each observation was divided into time bins of a size determined by the source intensity or by the time scale considered. Two statistical methods were used to test consistency with a constant emitter. For the LE data the first method used the χ^2 statistic,

$$\chi^2 = \sum_{i=1}^{N} \frac{(n_i - \mu_i)^2}{\mu_i} ,$$

calculated by dividing the data into time bins ($i = 1,.., N$). Here n_i is the total number of events detected (i.e., source + background) in the same box in which the source intensity was estimated, $\mu_i = \langle S \rangle t_i + b_i$ is the expected number of counts in the same box assuming a source of constant intensity equal to the mean value $\langle S \rangle$, measured during the whole observation; and t_i and b_i are the effective exposure time and the expected background. All the necessary corrections for telemetry and instrumental dead times have been included. In order to preserve the nature of the χ^2 statistic, time bins where the expected number of photons μ_i was less than 5 were not used.

For the ME data, where the uncertainty in the count rate is dominated by the background level,

$$\chi^2 = \sum_{i=1}^{N} \frac{(n_i - \mu_i)^2}{\sigma_{\mu_i}^2} ,$$

where n_i is the number of counts from source and background measured during bin i, and $\mu_i = \langle S \rangle t_i + b_i$ is the expected number of counts in the same time interval assuming a constant source; b_i is the number of background events, and t_i is the effective exposure time of bin i; $\langle S \rangle$ is the average source count rate as estimated during the entire observation.

The second method was the application of a Kolmogorov-Smirnov test to the expected and observed arrival time distributions of counts. This method is more efficient than the χ^2 test for the detection of secular trends in the data.

Several different time scales were probed, ranging from a few minutes to about 5000 s. The shortest time scales considered corresponded to an expected average of 10 source photons in each bin. Typical values are a few hundred seconds.

This method led to the detection of rapid variability, at a confidence level of 10^{-3}, in the eight objects discussed in turn below. These results were not sensitive to small changes in the bin widths.

i) *1H 0414+009*

Rapid variability of the ME flux from this object was found on 1984 days 253 (Fig. 6). The statistical significance of the event, however, is not high, and only the KS test gives a significant probability. Filter changes in front of the CMA detector prevented any detailed assessment of the simultaneous soft X-ray variability.

ii) *PKS 0548−322*

Significant rapid variability of the ME flux from PKS 0548−322 was found during the first and last *EXOSAT* observations of this object, in 1983 and 1986, respectively (Figs. 7*a* and 7*b*). The amplitude of the variability is only about 20%. In the CMA data no variability was found during the first observation, but during the second variability was detected with a significance of $\approx 10^{-4}$.

iii) *Mrk 421*

Rapid variability, of the order of 20%–30% in the ME data of Mrk 421, was detected on six occasions. On 1984 days 37, 337, 338, and 340, and on 1985 days 112 and 118 (Figs 8*a*–8*f*). In principle the count rate in the CMA was always sufficiently high for variability of this amplitude to be also resolved in the LE experiment. However, the several filter changes made resulted in no significant variation being detected in any of the observations.

iv) *ON 325*

ON 325 was observed by *EXOSAT* on 14 occasions either as a target or as a serendipitous source in the field of view of Mrk 766 or of 2A 1218+304. Rapid variability was observed on 1985 December 31 when ON 325 was detected $\approx 45'$ off-axis during a very long (≈ 57 hr) exposure of the Seyfert galaxy Mrk 766.

The CMA light curve of ON 325 during this observation is shown in Figure 9, where it can be seen that the source intensity decreased by a factor of about 3 in 15 ± 10 hr. No ME light curve is available because of source confusion due to the presence of Mrk 766 in the 90′ FWZI field of view of this nonimaging instrument.

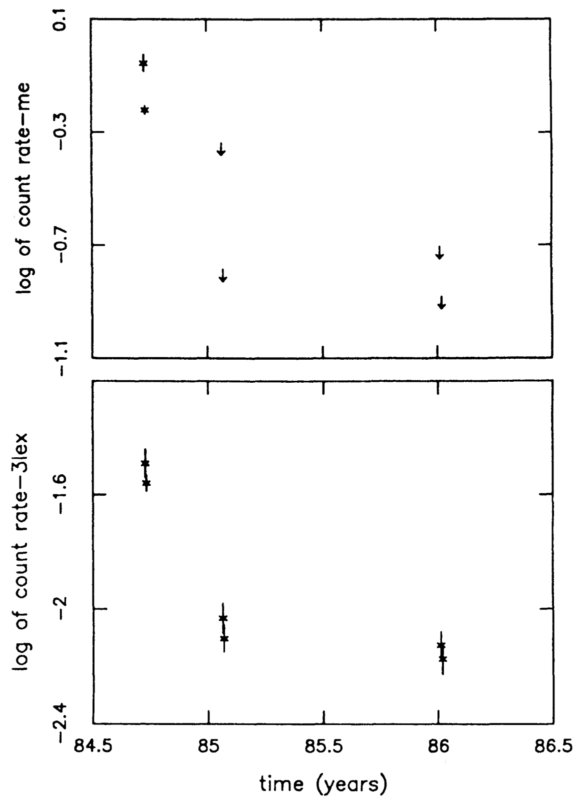

FIG. 5*a*

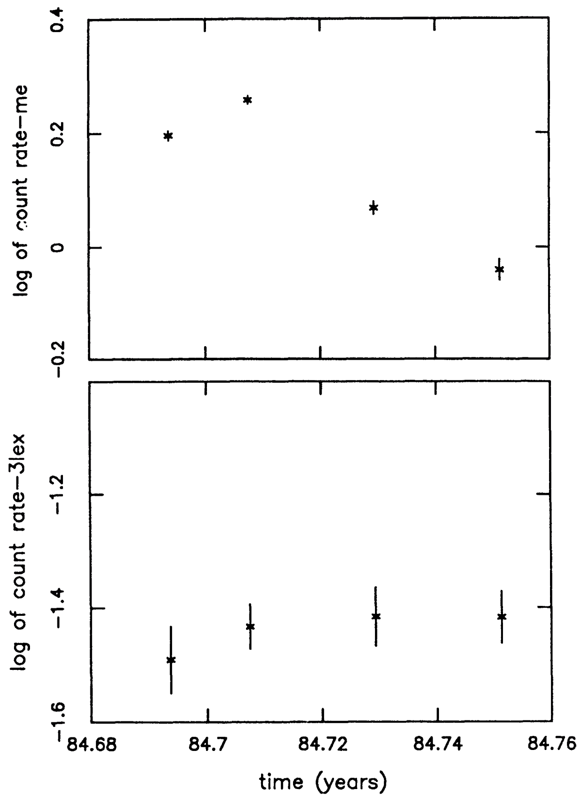

FIG. 5*b*

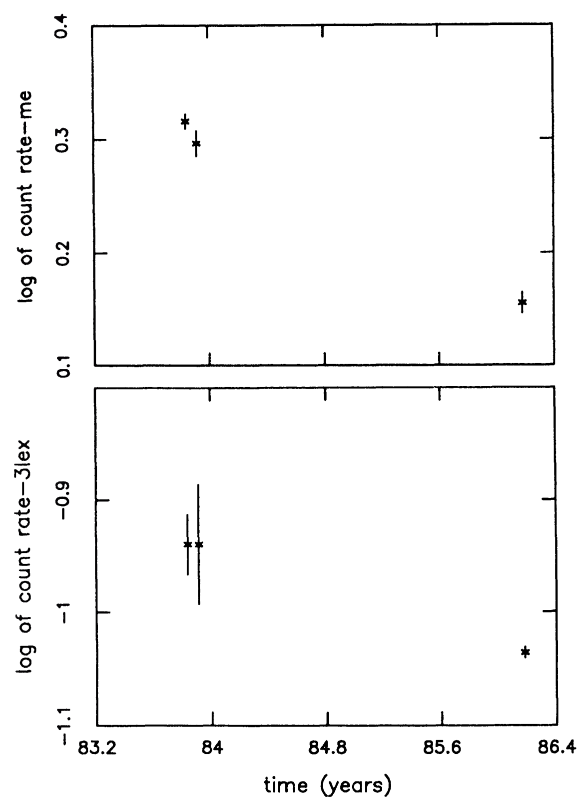

FIG. 5*c*

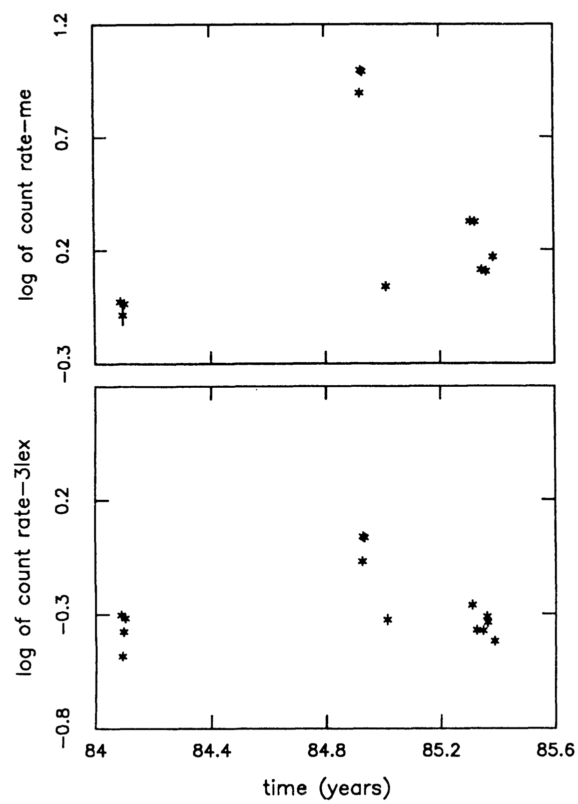

FIG. 5*d*

FIG. 5.—Simultaneous soft and hard X-ray light curves of all objects in the sample which were detected by both the CMA and the ME detectors. (*a*) 1H 0323+022, (*b*) 1H 0414+009, (*c*) PKS 0548−322, (*d*) Mrk 421, (*e*) Mrk 180, (*f*) Mrk 501, (*g*) PKS 2005−489, (*h*) PKS 2155−304. The scale on the *Y*-axis has been chosen so that equal separations between points in the soft and hard X-ray light curves correspond to the same flux variation.

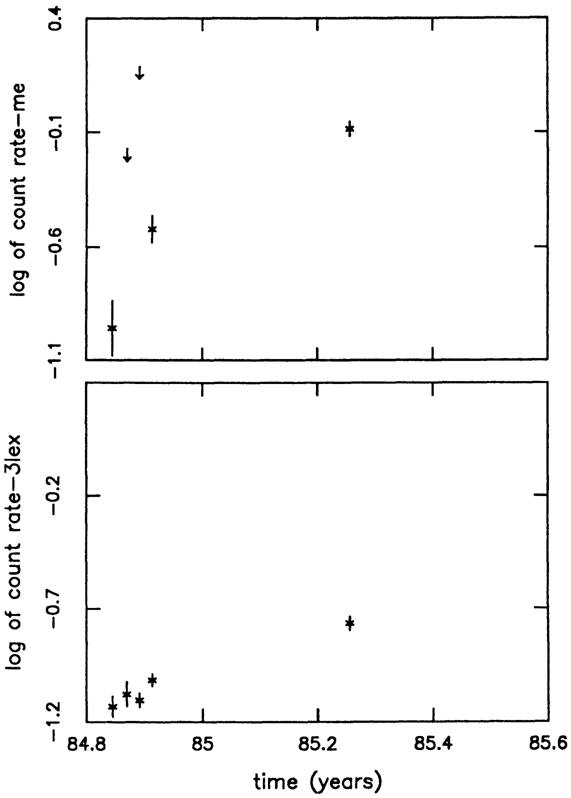

FIG. 5*e*

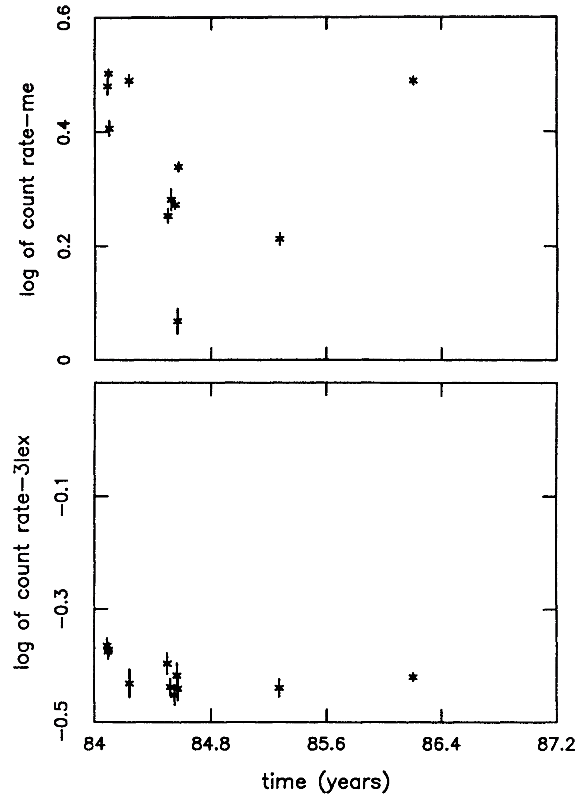

FIG. 5*f*

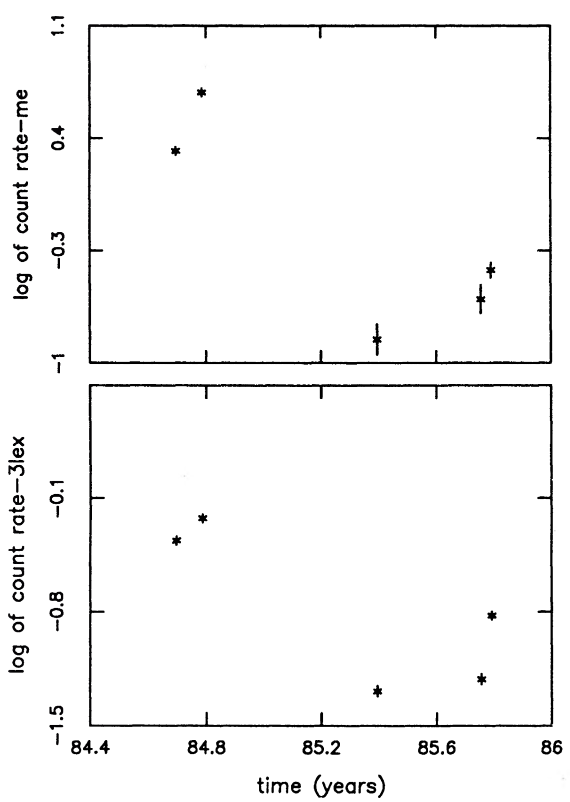

FIG. 5*g*

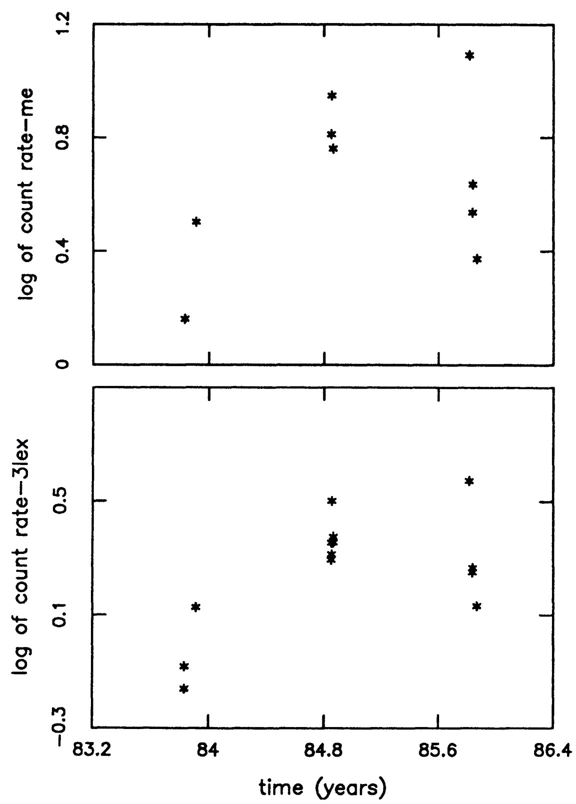

FIG. 5*h*

FIG. 5—*Continued*

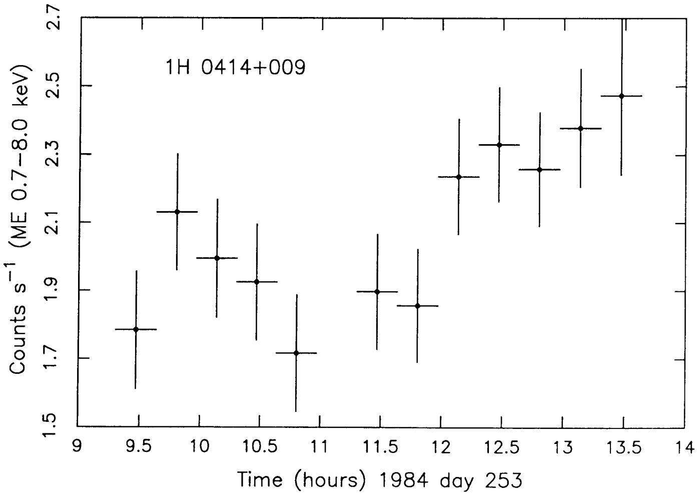

FIG. 6.—Short-term hard X-ray light curve of 1H 0414+009

The redshift of ON 325 is not known; therefore, no direct constraint on the geometry of the emitting region (e.g., Cavallo and Rees 1978; Fabian and Rees 1979) can be obtained. However, under the assumption of a Friedmann model of the universe with $q_0 = 0$ and $H_0 = 50$ km s^{-1} Mpc^{-1}, the observed variability is consistent with isotropic emission only if $z < 0.5$, for an assumed efficiency of conversion of matter into energy of $\eta = 0.1$.

The long-term soft X-ray light curve is shown in Figure 4*c*, where the episode of rapid variability described above appears as two points representing the source intensity at the beginning and at the end of the observation. During an exposure performed about two weeks later, the source was found essentially at the same level as at the end of the 1985 event. ON 325 remained approximately at the same intensity level for about two years, until the end of 1985, when it underwent a transition to the (lower) state, in which it was also observed 4 months later.

v) *1E 1402.3+0416*

A detailed analysis of all *EXOSAT* observations of 1E 1402.3+0416 has been presented in Giommi *et al.* (1986). We will not repeat it here; however, for completeness we recall that rapid variability of a factor of about 2 in a few hours was detected. The variability time scale is consistent with isotropic emission only if the redshift of this object is less than 0.2 (Giommi *et al.* 1986). The event of rapid variability is shown in the long-term CMA light curve of this object (Fig. 4*f*), where the count rates measured at the beginning and at the end of the first observation are plotted as separate points.

vi) *Mrk 501*

Variability of the order of 20%–40% of the hard X-ray flux was seen on 1986 day 74 (Fig. 10). Variations appear random on a time scale of a few hours. The simultaneous CMA light curve is consistent with that of a constant source. A 3 σ upper limit to soft X-ray variability on the same scale is less than 5%.

vii) *PKS 2005−489*

Among the objects in our sample, PKS 2005−489 showed the largest luminosity variability between different observations, with a maximum amplitude of factors of 11.5 ± 1 in soft X-rays (CMA + thin Lexan filter) and of 35 ± 7 in the 0.7–8 keV band. PKS 2005−489 also showed large-amplitude rapid variability in the ME band on two occasions, on 1985 October 3, when it increased its intensity by a factor of ≈4 in 4 hr (Fig. 11*a*), and 2 weeks later, when a decrease in flux, of approximately the same amplitude, occurred on a time scale of 4–5 hr (Fig. 11*b*). No significant varibility could be found in the CMA data. As in several other cases, variability analysis is complicated by the filter changes that were made during both observations. The count-rate ratio in the thin Lexan and aluminum-parylene filters is consistent with a constant source, whereas the count rate in the boron filter, used toward the end of the second observation, is substantially lower than expected on the basis of the source intensity in the thin Lexan and aluminum-parylene filters assuming a power-law spectrum with slope $\alpha < 1.5$ and no intrinsic absorption. The redshift of PKS 2005−489 is not known; the above results do not imply special or relativistic effects only if $z < 0.17$, assuming $\eta = 0.1$.

viii) *PKS 2155−304*

Detailed analysis of PKS 2155−304 has been presented in Morini *et al.* (1986), Treves *et al.* (1989), and Tagliaferri *et al.* (1989*b*). The hard and soft X-ray light curves of all observa-

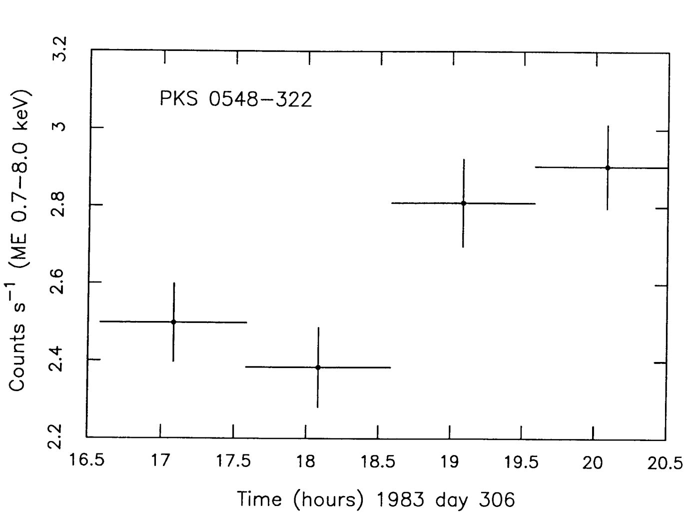

FIG. 7*a*

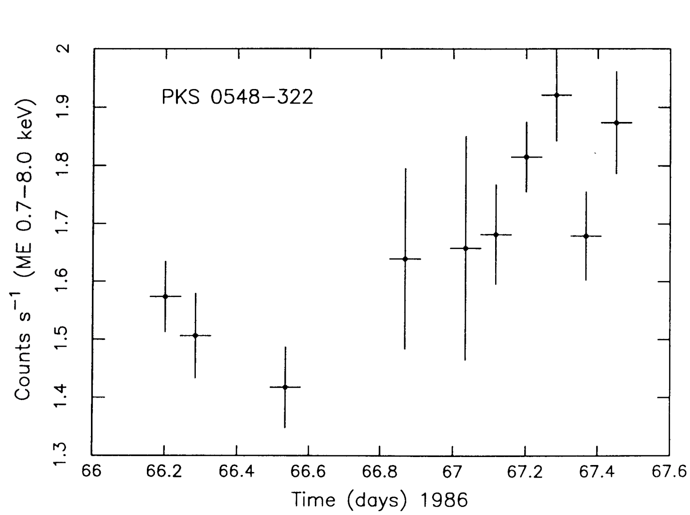

FIG. 7*b*

FIG. 7.—(*a*, *b*) Short-term hard X-ray light curves of PKS 0548−322

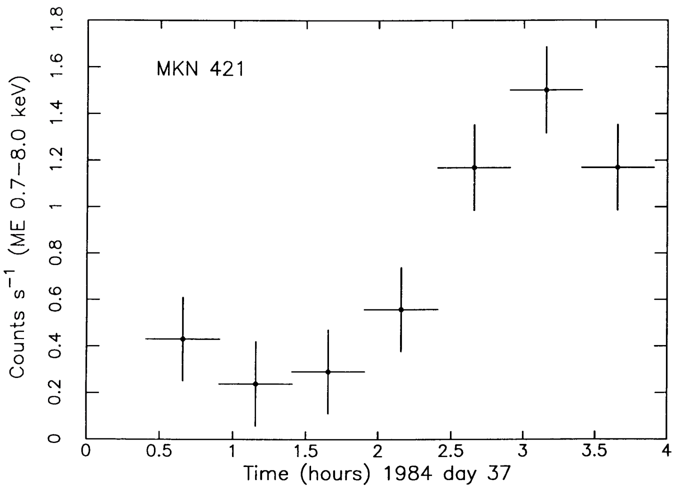

FIG. 8*a*

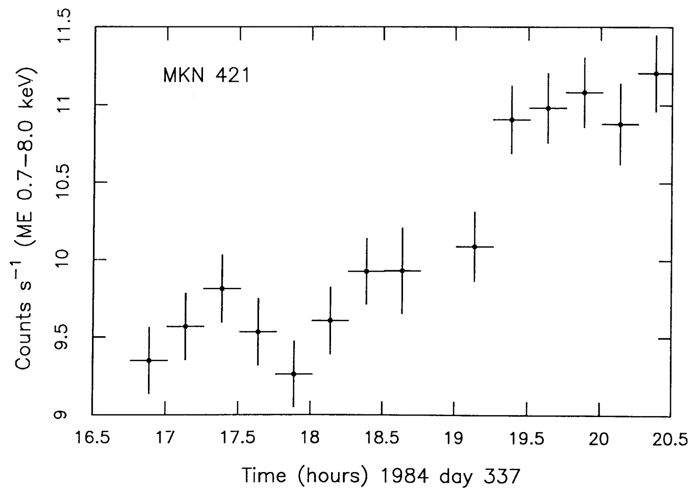

FIG. 8*b*

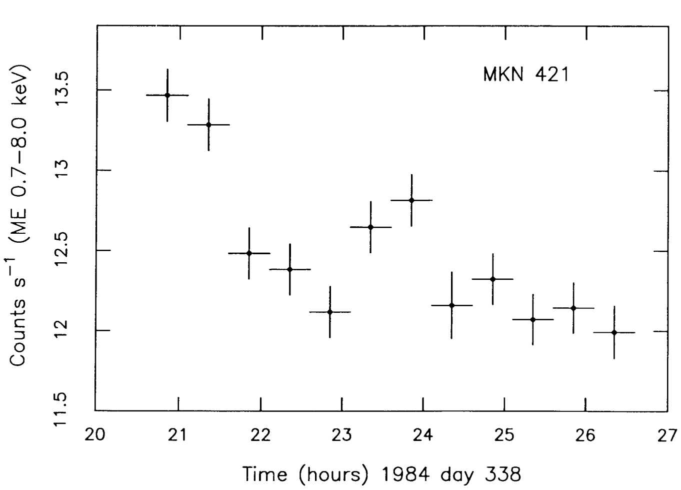

FIG. 8*c*

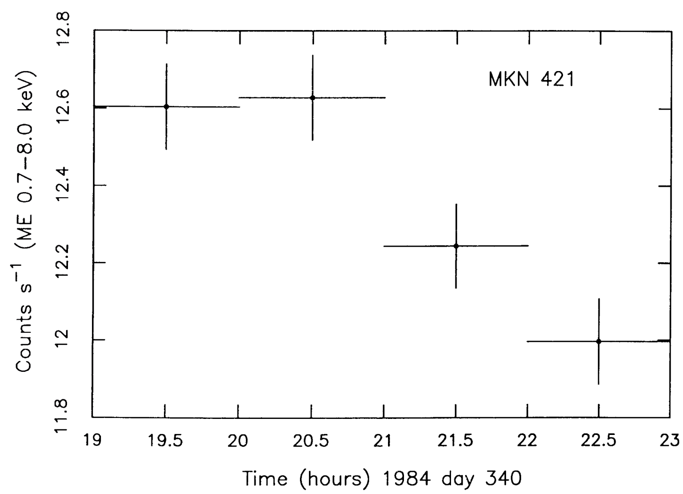

FIG. 8*d*

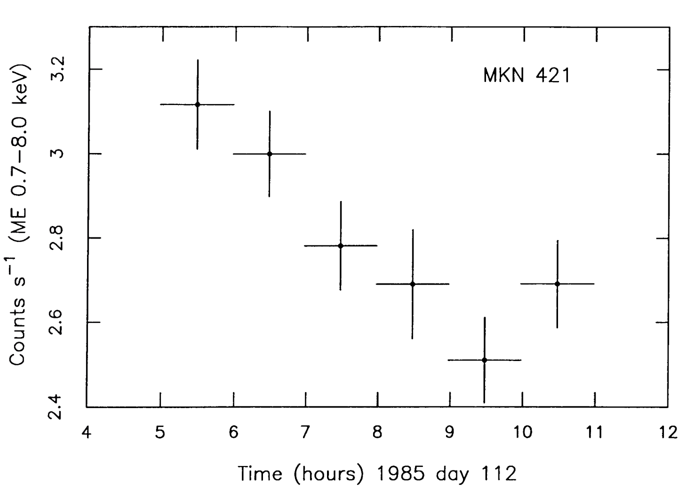

FIG. 8*e*

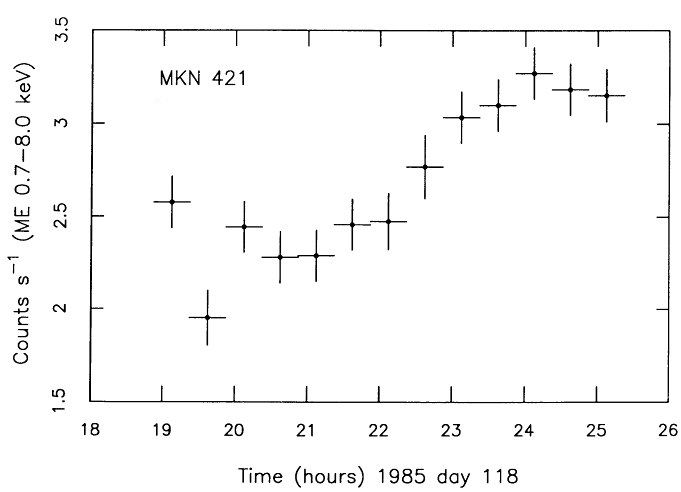

FIG. 8*f*

FIG. 8.—(*a–f*) Short-term hard X-ray light curves of Mrk 421

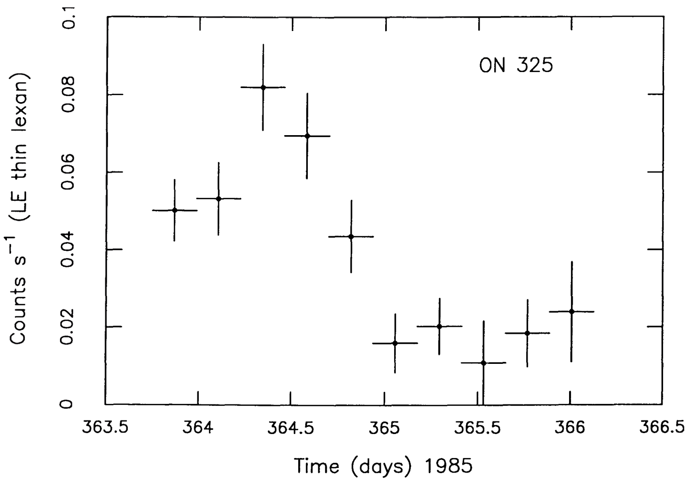

FIG. 9.—Short-term soft X-ray light curve of ON 325

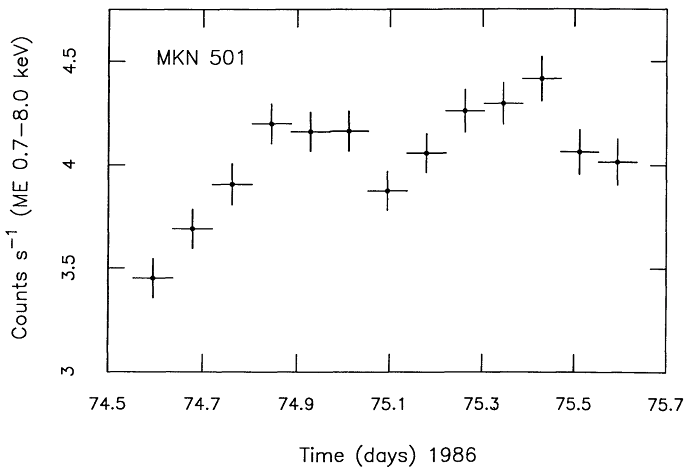

FIG. 10.—Short-term hard X-ray light curve of Mrk 501

tions where this object was found by our analysis to be variable are shown in Figures 12*a*–12*f* and 13*a*–13*d*. Filter changes performed while the ME flux was varying complicate the analysis of the CMA data and give no useful constraints on the level of soft X-ray variability. Strong variability of up to a factor of 4 during single observations was detected on three occasions, on 1984 days 311 and 312 and 1985 day 316 (Figs. 12*a*, 12*b*, 12*f*, and 13*b*, respectively). During the first two of these observations the flux showed rapid regular rising with a doubling time of 1–2 hr. The minimum time scale variability implies relativistic amplification of the observed radiation with a kinematic Doppler factor $\delta \approx 2$–3. On 1985 day 297 PKS 2155−304 regularly decreased both its ME and LE intensity until approximately 20:00 UT, when the source intensity started rising again and rose until the end of the observation, when it almost reached the same level measured at the beginning of the exposure (Figs. 12*d* and 13*c*). On 1983 day 304 both the χ^2 test and the KS test find significant variability (with the probability that the source is constant equal to 2×10^{-12} and 6×10^{-6}, respectively) in the CMA light curve (Fig. 13*a*), while the ME flux was consistent with a constant source.

c) Spectral Variability

A complete analysis of the spectral properties of all BL Lacs in the sample that were detected with sufficient statistics in the ME experiment will be reported elsewhere (Barr *et al.* 1989*a*; for a preliminary analysis see Barr *et al.* 1989*b*). Here we study the spectral variability through changes of the sources' hardness ratio with intensity. In Figures 14*a*–14*f* the hardness ratio (defined as the ratio between the average ME count rate and the average count rate in the CMA + thin Lexan filter) is plotted as a function of intensity in the 0.7–8 keV band for all the brighter sources which were not confused in the ME experiment namely, 1H 0414+009, Mrk 421, Mrk 180, Mrk 501, PKS 2005−48, and PKS 2155−304. In each case the hardness ratio increases significantly with intensity, implying that the sources' spectra harden as their fluxes increase. The same behavior is probably also present in PKS 0548−322 and 1H 0323+022.

A correlation between spectral slope and source intensity was noted by Morini *et al.* (1986), George, Warwick, and Bromage (1988), and George, Warwick, and McHardy (1989).

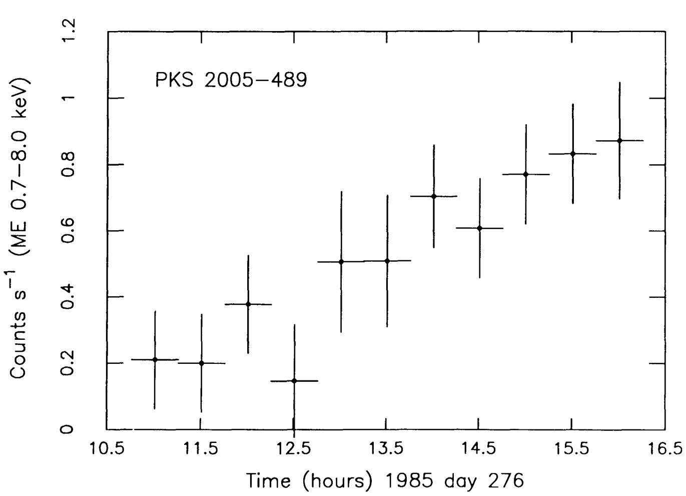

FIG. 11*a*

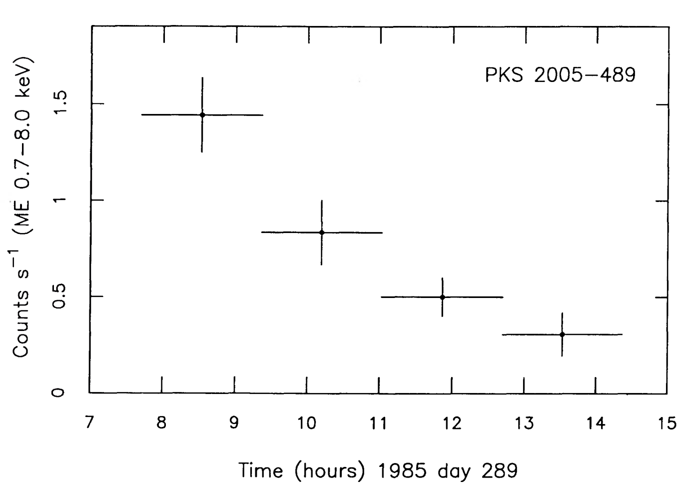

FIG. 11*b*

FIG. 11.—(*a*, *b*) Short-term hard X-ray light curves of PKS 2005−489

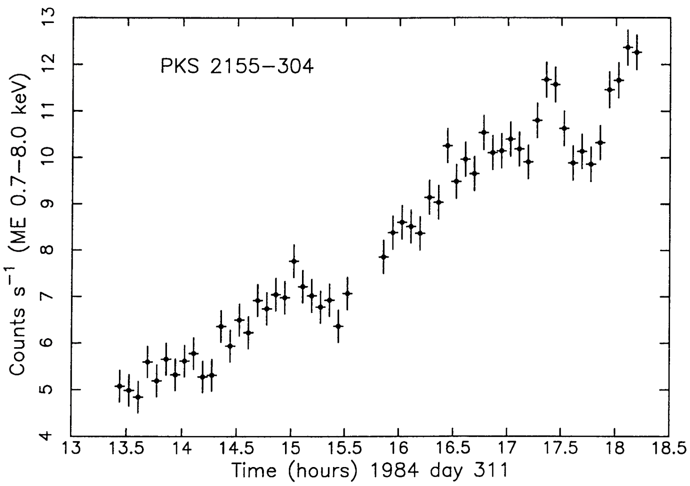

FIG. 12*a*

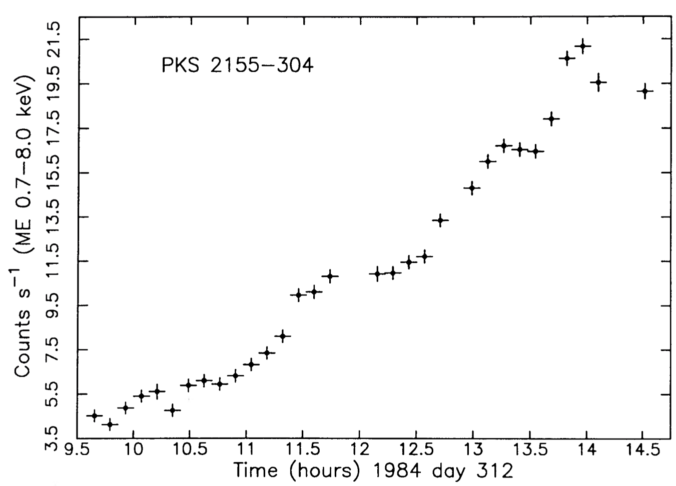

FIG. 12*b*

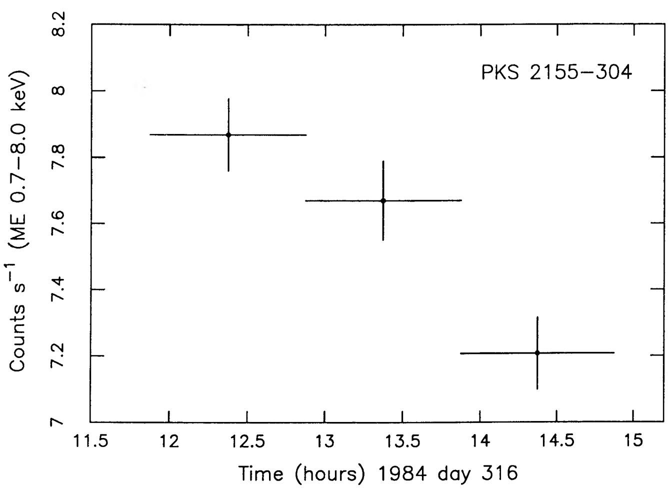

FIG. 12*c*

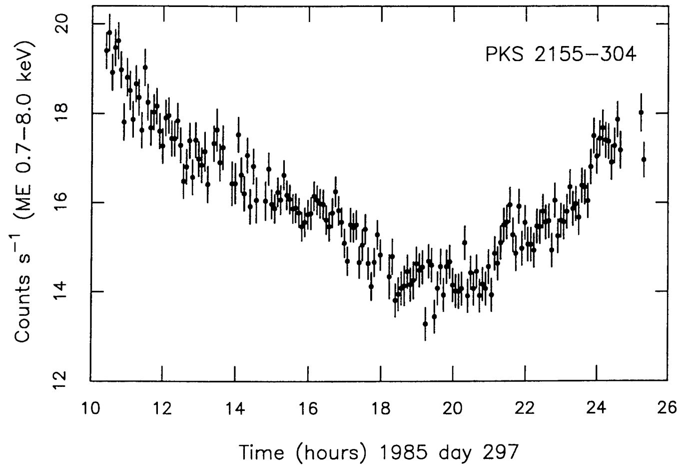

FIG. 12*d*

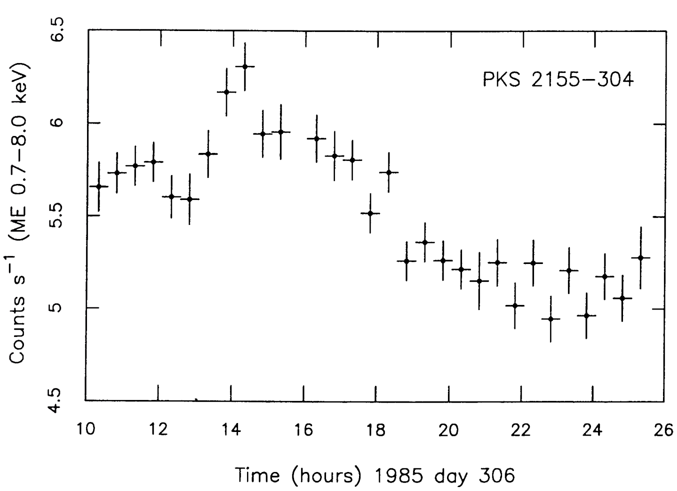

FIG. 12*e*

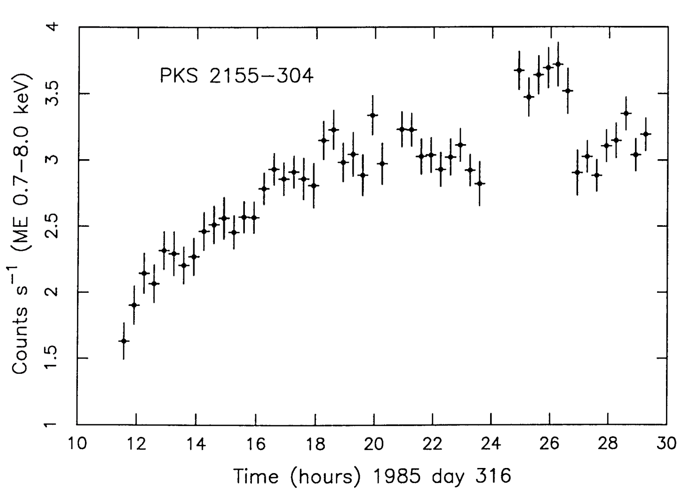

FIG. 12*f*

FIG. 12.—(*a–f*) Short-term hard X-ray light curves of PKS 2155−304

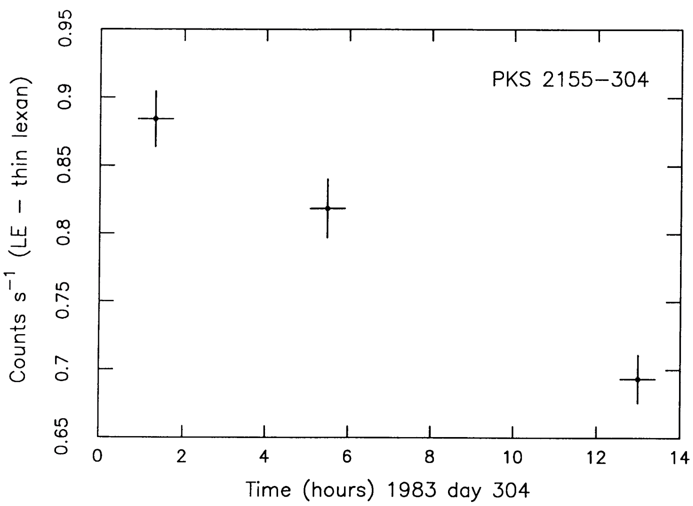

FIG. 13*a*

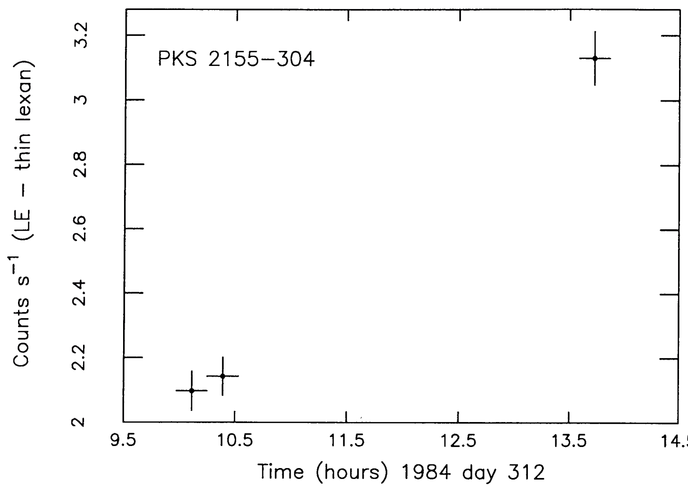

FIG. 13*b*

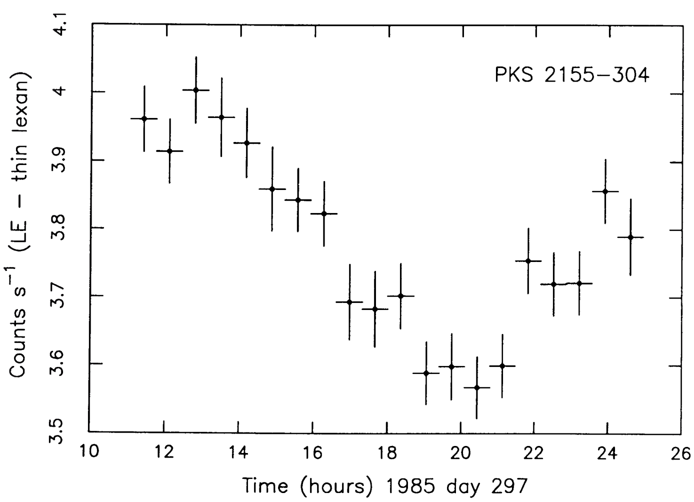

FIG. 13*c*

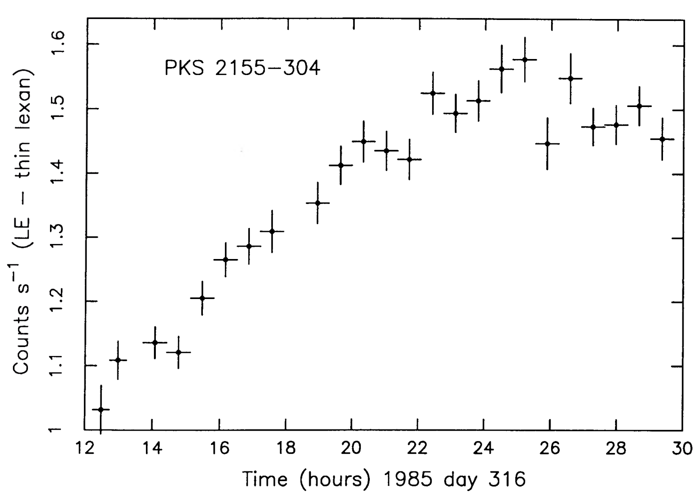

FIG. 13*d*

FIG. 13.—(*a*–*d*) Short-term soft X-ray light curves of PKS 2155−304

Our results show that this behavior is very common and could be a distinguishing characteristic of BL Lac objects. For Mrk 421 the hardness ratio increases linearly with source intensity until it saturates at a constant value above a count rate of ≈ 5 count s^{-1} (see Fig. 14*b*). The same behavior is present in PKS 2155−304 (Fig. 14*f*), although with a larger scatter due to the large rapid variability seen during some observations.

The only objects which we were able to study in this way are X–BL Lacs; therefore, it is not known whether Q–BL Lacs show similar spectral changes.

The wide range of hardness ratios in different objects is to some extent a reflection of the amount of the interstellar absorbing material toward each object. Ideally the hardness ratio should refer to absorption-corrected count rates. However, this would require a detailed knowledge of the individual intrinsic energy spectra at the time of the event, which are generally not available.

VII. THE LUMINOSITY VARIABILITY FUNCTION

In most cases, the light curves of Figures 4*a*–4*h* and 5*a*–5*h* reveal common types of behavior. First, there is no evidence for long-term trends in the X-ray emission in any of the objects that were well monitored. Second, the variability does not appear to be random, as can be seen from the distribution of the count rates about the average intensity in each source. This distribution is not symmetric but is skewed toward high values of the count rate (skewness = 2.64). In the most cases the data are consistent with X-ray emission that fluctuates about a level that remains constant over periods of the order of years, with rapid and sometimes large-amplitude variability superposed. This behavior is most marked in the LE experiment.

In order to study the time variability of BL Lacs as a class, we will now assume that all BL Lacs in our sample behave in the same way. Before proceeding, however, we must make a short digression to discuss some of the statistical properties of the sample.

The set of observations considered includes all the pointings of BL Lac objects listed in the Burbidge and Hewitt (1987) catalog that are available in the *EXOSAT* archive. Therefore, it is not statistically well defined and not necessarily unbiased. In addition, the sampling of the light curves is uneven. In a few cases X-ray observations were made as targets of opportunity

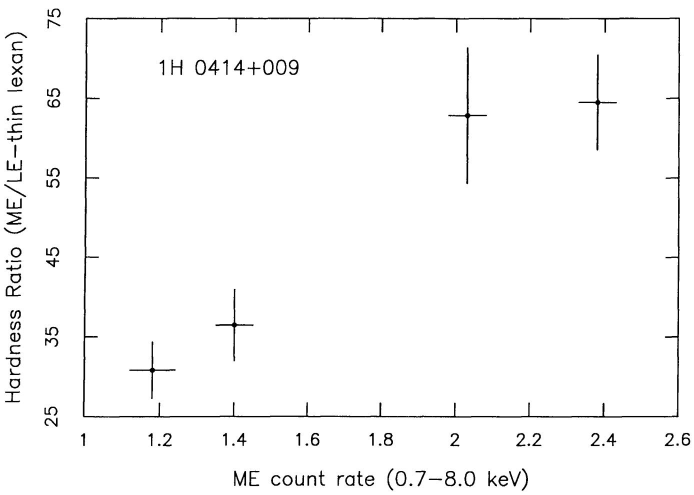

FIG. 14*a*

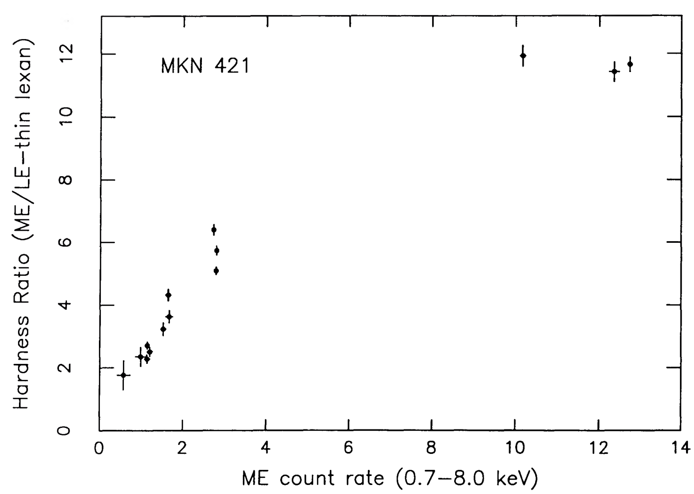

FIG. 14*b*

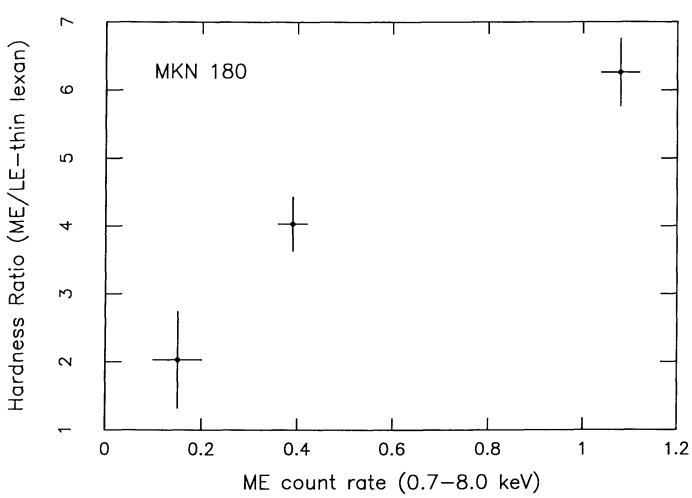

FIG. 14*c*

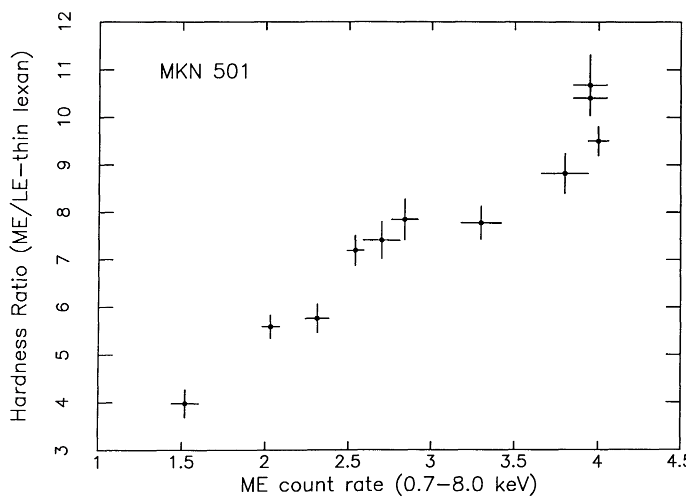

FIG. 14*d*

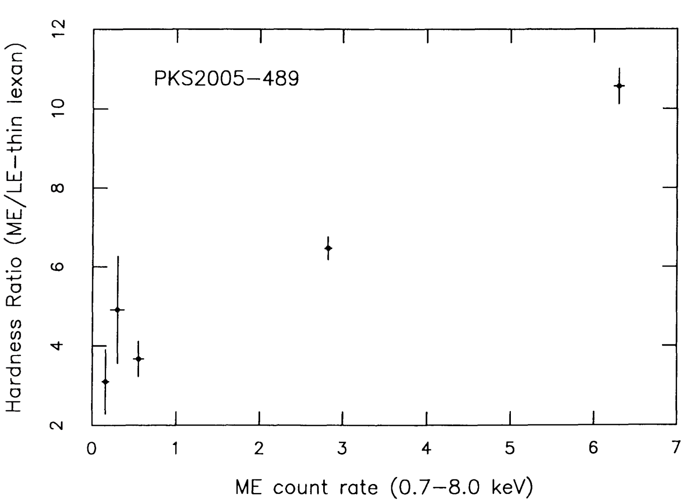

FIG. 14*e*

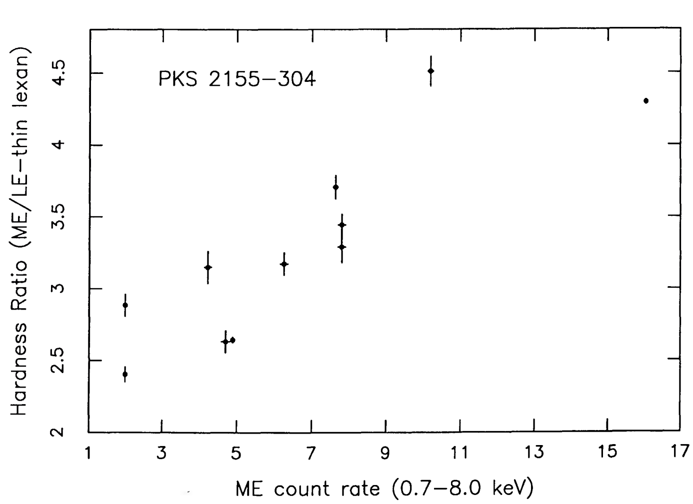

FIG. 14*f*

FIG. 14.—X-ray hardness ratio, defined as the count rate in the ME instruments and the count rate in the CMA plus thin Lexan filter, plotted as a function of hard X-ray intensity for the cases of (*a*) 1H 0414+009, (*b*) Mrk 421, (*c*) Mrk 180, (*d*) Mrk 501, (*e*) PKS 2055−489, (*f*) PKS 2155−304.

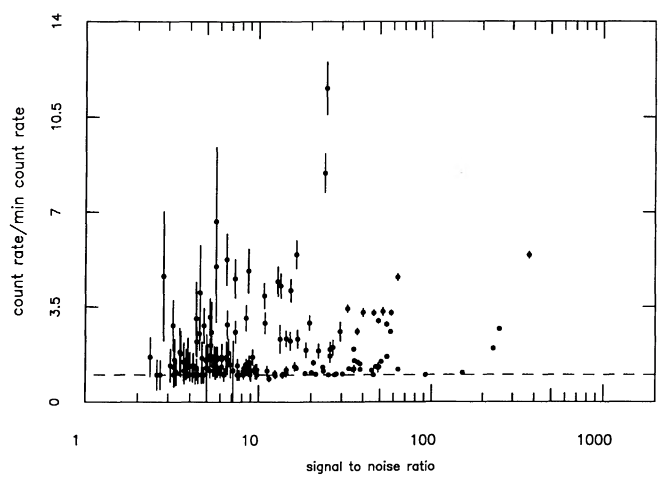

FIG. 15.—Ratio of the measured count rate to the minimum observed count rate in the same source plotted against signal-to-noise ratio for all BL Lacs detected at least 3 times by the CMA plus thin Lexan filter.

following the results of observations made at some other frequency (usually optical) which showed that an object was especially bright. This clearly results in a bias unless the time scale of the variability is much smaller than the reaction time to carry out an observation as a target of opportunity (usually one day). In one case (1E 1402.3+0416) observations were repeated shortly after the source was found by *EXOSAT* to be in a high state, thus departing again from the random sampling necessary for a proper statistical study of time variability. Bearing in mind these limitations, we can now attempt to study the X-ray variability of BL Lacs as a class.

Figure 15 is a plot of the ratio between the count rate measured by the CMA and thin Lexan filter during each observation and the minimum count rate observed in the same source as a function of signal-to-noise ratio. Variability of up to factors of about 6–10 is present independently of the signal-to-noise ratio. From Figure 15 it is clear that small-amplitude variations occur much more frequently than large flares. In order to estimate the frequency with which variations of a given amplitude occur, we have to face a problem. While very large amplitude variations could easily have been detected in all the objects, variations of the order of a few percent could have been detected only in the limited number of cases where the signal-to-noise ratio was sufficiently high. The simplest way of avoiding this problem is to consider only the bright objects, for instance, those detected with a signal-to-noise ratio greater than 10. However, this would exclude the majority of the observations from the analysis, with the consequent loss of the information contained in the upper limits to variability. In order to make use of all the information available, we have applied a method that was originally derived for the estimation of the radio luminosity function of a sample of spiral galaxies in the presence of upper limits to the radio flux (Hummel 1981). The problem here is similar, in that we want to estimate the fraction of time that BL Lacs spend away from some reference level, L_*, which is equivalent to estimating the fraction of galaxies with radio luminosity in a given luminosity interval. Some of the galaxies are too faint in the radio to be detected, in the same way that some or our BL Lacs are too faint for a small $\delta L = (L - L_*)/L_*$ to be detected. Upper limits to the radio luminosity and to luminosity variability can be derived in both cases. By analogy with the case of the luminosity function, we call the relation that the fraction of time that BL Lacs spend away from the reference level L_* the luminosity variability function (LVF). In order to calculate the LVF we divide the δL axis in to bins so that a given variation δL belongs to bin k if $|\delta L_k| - \Delta_k < |\delta L| \leq |\delta L_k| + \Delta_k$, where δL_k and $2\Delta_k$ are the center and the width of bin k, respectively. Following Hummel (1981), we have

$$f_k = \frac{n_{\mathrm{det}_k}(1 - \sum_{j=0}^{k-1} f_j)}{n_{\mathrm{ul}}(|\delta L| < |\delta L_k| - \Delta_k) + n_{\mathrm{det}}(|\delta L| \leq |\delta L_k| + \Delta_k)} ,$$

$$f_0 = 0 ,$$

$$\delta L = \frac{L - L_*}{L_*} , \quad |\delta L_i| < |\delta L_k| \quad \text{for } i > k .$$

With this definition the LVF is normalized:

$$\sum_{j=0}^{\infty} f_j = 1 .$$

In the expression for f_k, n_{ul} is the number of upper limits (defined as 3 times the statistical noise of the observation) to variations of amplitude $|\delta L_i|$ and n_{det} is the number of significant detections of variability with amplitude $|\delta L|$ included in bin k. For our calculations we have considered only objects that were detected at least 3 times, and we have taken as reference level L_* each source's medium count rate. The medium rather than the mean was chosen to represent L_* because it has the advantage of being close to the quiescent level in cases such as Mrk 421, where the source remains close to a minimum level and occasionally flares, while it becomes very close to the mean where no variability is seen.

The LVF so derived is shown in Figure 16 for the case of LE data. The LVF is a fairly steep function of $|\delta L|$, implying that small variations occur much more frequently than large outbursts. The average BL Lac spends about 90% of its time

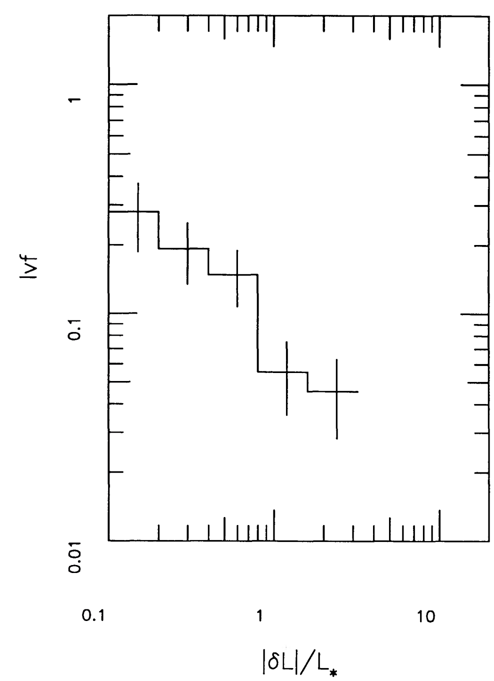

FIG. 16.—Soft X-ray luminosity varability function of BL Lac objects (see text for details).

within a factor of 2 of the quiescent flux, and only a very small fraction of the time flaring.

Because of the limitations and because of possible inhomogeneities in the sample and the limited number of observations, the LVF of Figure 16 is only an approximation to the true LVF of BL Lacs. It may well be that different BL Lacs are characterized by different LVFs. Indeed, even within the limitations of the current work, the two objects 1E 1207.9+3945 and 1E 1415.6+2557 appear unusually stable. Obviously a large number of long and uninterrupted observations of each BL Lac in the sample would be ideal for this study. It goes without saying that we are far from that.

VIII. INTRINSIC ABSORPTION

The very low energy bandpass of the *EXOSAT* telescopes (0.05–2.0 keV), combined with the different transparency to X-ray photons of the filters available, make this instrument particularly well suited to study the intrinsic absorption in BL Lacs. In particular, the ratio between the count rates observed in two different filters for a given constant source provides information on the total amount of equivalent N_H along the line of sight.

Detections in more than one filter have been achieved in 21 of the objects of the sample. In some cases, however, the source was detected just above the sensitivity limit, and the uncertainty in the count-rate ratio is unacceptably large. In addition, in a few instances the source flux varied significantly during the observation, thus making the count-rate ratio an unreliable estimate of the amount of N_H. Such measurements were not used in the following analysis. In Figure 17 the ratio of the count rates in the 3000 Å Lexan and aluminum-parylene filters of 50 observations of the 14 objects that were sufficiently bright to allow an estimate of the count-rate ratio with a small error is plotted as a function of the amount of the Galactic N_H along the line of sight as estimated from the 21 cm measurements of Stark *et al.* (1990). The solid lines represent the expected value of the count-rate ratio for no intrinsic absorption and for two values of the spectral index ($\alpha = 1$ and $\alpha = 2$; $F_\nu \propto \nu^{-\alpha}$). The dashed lines represent the expected values of

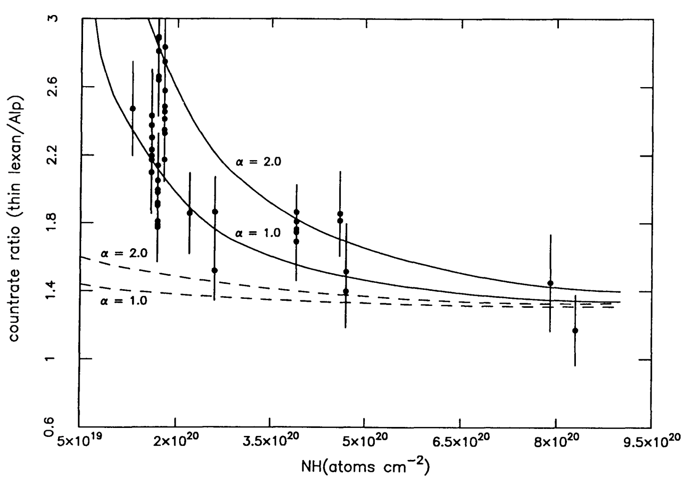

FIG. 17.—Ratio of the count rates in the thin Lexan and aluminum-parylene filters of 50 observations of 14 BL Lacs, plotted as a function of Galactic N_H. Solid lines represent the expected ratios assuming no intrinsic absorption for the cases of source energy spectral slope $\alpha = 1$ and $\alpha = 2$. Dashed lines are the corresponding curves assuming an intrinsic absorption equivalent to $N_H = 5 \times 10^{20}$ atoms cm^{-2}.

the count-rate ratios assuming an intrinsic absorption of 5×10^{20} atoms cm^{-2}, again for $\alpha = 1$ and $\alpha = 2$. It is clear from Figure 17 that the measurements are always in good agreement with the solid lines and in poor agreement with the dashed lines strongly suggesting little or no intrinsic absorption due to cold material.

IX. DISCUSSION

Our results provide further strong evidence that the population of currently known BL Lac objects can be divided into two subclasses, Q–BL Lacs and X–BL Lacs, which are characterized by different intrinsic energy distributions. This classification is preferable to the common practice of dividing BL Lacs into radio-selected and X-ray–selected objects because it is based on intrinsic rather than observational properties, and is therefore independent of the method by which the sources were originally discovered.

The subclass of Q–BL Lacs includes most of the classical, radio-discovered, BL Lac objects which are characterized by a continuum energy distribution, from radio to X-rays, similar to that of flat-radio-spectrum QSOs, highly polarized quasars (HPQs), and optically violent variable QSOs (OVVs). This similarity suggests a continuity between Q–BL Lacs and other types of radio-emitting active galactic nuclei supporting the picture where all these objects are grouped under the name of blazars. We note, however, that significant differences in the X-ray spectral index have been found between a sample of radio-selected BL Lacs and samples of HPQs and OVVs (Worrall 1989).

The subclass of X–BL Lacs includes all the BL Lac objects which were detected in high-frequency surveys (i.e., optical and X-ray). X–BL Lacs are characterized by a very smooth energy distribution from radio to X-rays, which is often considered to be the signature of synchrotron emission (e.g., Ghisellini *et al.* 1986).

The soft X-ray log N–log S curve obtained with both *Einstein* and *EXOSAT* data predicts that during the *ROSAT* all-sky survey (Trümper 1984) a few thousand new BL Lacs will be found. Since essentially none of the BL Lacs so far discovered in X-ray surveys are Q–BL Lacs, X–BL Lacs are expected to vastly outnumber Q–BL Lacs when the results of the *ROSAT* survey are available. In addition, since the X-ray luminosity of Q–BL Lacs is similar to that X–BL Lacs, these last must be *intrinsically* more abundant then Q–BL Lacs (see also Maraschi *et al.* 1986).

Although the *ROSAT* all-sky survey will dramatically increase the number of the known BL Lacs, the combination of the observed X-ray log N–log S relation and the correlations between the optical and X-ray flux suggest that these sources will remain comparatively rare, with a density of one object every 20–30 square degrees of sky at $m_v < 19$–20 (Maccacaro *et al.* 1989; Giommi *et al.* 1989*a*).

The correlations between radio, optical, and soft X-ray flux found in the population of X–BL Lacs imply that different parts of the electromagnetic spectrum of these sources are directly related, supporting emission models where radiation at different frequencies is generated by processes which are not independent. The situation appears more complicated in the case of Q–BL Lacs, where no correlations have been found. A regression analysis performed on a sample of 30 BL Lacs extracted from the *Einstein* EMSS (Maccacaro *et al.* 1989) confirms the correlations between the optical and radio fluxes and between the X-ray and radio fluxes present in the sample of

X–BL Lacs studied in this paper with a confidence above 99.5%. However, a larger scatter is seen in the EMSS data. This could possibly be explained by the variability, since, in general, only one estimate of the optical, radio, and X-ray flux of each EMSS source is available, and this has been used for the regession analysis, while the minimum of often several measurements was used for the analysis of our sample. This interpretation is supported by the fact that if the intensities used to construct Figures 2*a* and 3*a* are chosen at random, among different observations of each source, the amount of scatter increases.

The extrapolation of the correlation between X-ray and radio fluxes found for the subsample of X–BL Lacs to fluxes[5] $< 1 \times 10^{-12}$ ergs cm^{-2} s^{-1} implies expected radio flux densities of ≈ 3 mJy or less (see Fig. 2*a*) and corresponding optical apparent magnitude greater than 20 (Fig, 3*a*). Consequently, X–BL Lacs with *observed* soft X-ray flux less than 5×10^{-13} ergs cm^{-2} s^{-1} are particularly difficult to identify. A further complication is that they might be at the center of a bright elliptical galaxy and could therefore be outshone by the light of the galaxy's stellar population.

In several models of BL Lac emission, electromagnetic radiation is produced via the synchrotron process, by electrons possibly located in different regions and characterized by different energy distributions (e.g., Ghisellini and Maraschi 1989), from radio up to a maximum frequency generally located between the optical and the X-ray band. Above this frequency the spectrum steepens considerably because of energy losses. Substantial emission at higher energies would be still possible via inverse Compton or other mechanisms.

Spectral breaks in the X-ray domain have been detected in some X–BL Lacs (PKS 0548−322: Madejski 1985, Barr, Giommi, and Maccagni 1988; Mrk 421: Barr *et al.* 1989*b*; PKS 2005−48: Barr *et al.* 1989*b*; and possibly 1E 1415−2557: Giommi *et al.* 1987) and at lower frequencies in BL Lac itself (Bergman *et al.* 1990) and in other Q–BL Lacs (Tanzi *et al.* 1989; Falomo *et al.* 1989). In addition, the presence of spectral curvature somewhere between the optical and the soft X-ray band is also implied by the steep spectral indices often found in hard X-rays and by the distribution of the optical to X-ray spectral slope, α_{ox}, which shows that values of ≈ 1 or smaller are much more frequent than steeper values. Madejski and Schwartz (1989), in spectral study of the *Einstein* sample of BL Lacs, using IPC and MPC data, also concluded that "X-ray spectra of BL Lacs must systematically steepen in the 1–3 keV band." Ghisellini *et al.* 1986, in a study of the radio to X-ray spectral characteristics of a sample of Blazars observed with *IUE*, reached the conclusion that the dominant emission in their small subsample of six X-ray–selected BL Lacs is synchrotron from radio to X-rays, whereas some contribution from Compton emission must be present in the X-ray spectrum of radio-selected objects, after a break in the synchrotron emission at lower energies.

A variety of spectral break energies, ranging from the optical to X-rays, may therefore exist in BL Lacs. Under the assumption that synchrotron emission before the break is the dominant source of radiation, X-ray selection strongly favors the discovery of objects where the break is located close to the X-ray band or above. The observed spectrum from radio to X-rays of these sources would then be almost pure synchrotron, and their energy distribution would be very similar to that of X–BL Lacs. The Crab Pulsar, which is widely recognized as a synchrotron emitter, is characterized by $\alpha_{ro} \approx 0.37$ and $\alpha_{ox} \approx 0.9$, and is well within the area of the α_{ro}-α_{ox} diagram (Fig. 1) occupied by X–BL Lacs (Baldwin 1971; Urry 1986).

If there are BL Lacs with the break in the optical or in the UV band, they would be much less intense sources of synchrotron X-rays, although they could still be detectable because of inverse Compton emission. These sources could in principle be even more abundent then the presently known population of BL Lacs. Moderate-sensitivity X-ray surveys, such as the *HEAO 1* (Schwartz *et al.* 1989), the EMSS (Gioia *et al.* 1990), and the *EXOSAT* HGLS (Giommi, Tagliaferri, and Angelini 1988; Giommi *et al.* 1989*a*), which preferably select sources where the break is close to or above the X-ray band, could then simply be showing the tip of the iceberg. When high-sensitivity and large-area X-ray surveys become available, a large number of BL Lacs characterized by break eneergies in the optical/UV part of the spectrum could be discovered if the spectrum above the break is not too steep.

The high radio emission of Q–BL Lacs is explained by Maraschi *et al.* (1986) and Ghisellini and Maraschi (1989) within a model where radio emission is highly beamed, while radiation at higher energies is less beamed. In this scenario Q–BL Lacs would be those very rare objects where the radio beam points toward us , while the remaining objects, i.e., those characterized by any beam direction and by any break energy, would constitute their "parent population." The volume density of the underlying (or "parent") population of BL Lacs could therefore be as high as or higher than that of other types of AGNs. If this were the case, it would be ironic that the rare radio-strong Q–BL Lacs were discovered first, the more abundent X–BL Lacs were discovered several years later, while the vast majority of the population is yet to be discovered.

If there is an underlying population with a variety of spectral break energies, strong *K*-correction effects lead to the prediction that moderate-sensitivity X-ray surveys preferentially select nearby objects and that the resulting X-ray log *N*–log *S* curve can significantly deviate from that expected for a uniform distribution of sources. This might explain the surprisingly flat X-ray log *N*–log *S* curve of BL Lacs derived from the *Einstein* and the *EXOSAT* serendipitous surveys (Maccacaro *et al.* 1984; Giommi *et al.* 1989*a*). At lower flux limits than the *Einstein* EMSS, many more BL Lacs than expected could then be discovered if an extra component of X-ray emission, due to, e.g., inverse compton or another mechanism, dominated synchrotron emission at higher energies, and the log *N*–log *S* curve could rise steeply. At these faint fluxes, because of the different emission mechanisms involved, X-ray–discovered BL Lacs might not be confined to a small area of the α_{ro}-α_{ox} diagram any more, and the clear distinction between Q–BL Lacs and X–BL Lacs may start to blur.

Luminosity variability with amplitudes from $\approx 10\%$ to about a factor of 30 has been detected in 16 objects, strongly confirming that BL Lac objects are highly variable X-ray sources as a class.

No evidence for long-term trends in the light curve of any object has been found, indicating that flux variability is probably due to short events, lasting hours or days, above a quiescent level that remains approximately constant over time scales of the order of years. Variability between observations more than a few days apart probably then represents unrelated intensity states in which the objects happened to be found.

[5] This flux is corrected for Galactic absorption and corresponds to an observed flux of $\approx 4 \times 10^{-13}$ ergs cm^{-2} s^{-1} for a power-law spectrum with energy slope of 1.0 and $N_H = 4 \times 10^{20}$ atoms cm^{-2}.

Since variability time scales in the X-ray band are so short, comparison between intensity variations at different frequencies must be treated with great care to avoid comparing unrelated events. Safe information about times lags in different energy bands can therefore be extracted only from observations of sufficient length that are strictly simultaneous.

Flux changes between different observations were detected in four out of 10 objects belonging to the Q–BL Lac class and in 12 out of 16 objects of the X–BL Lacs. Although the percentage of objects that showed significant variability is higher among X–BL Lacs, we cannot consider this as strong evidence that objects belonging to this class are more variable than Q–BL Lacs, since the latter are in general weaker X-ray sources and were observed less often. The data available simply do not allow us to detect significant differences between the X-ray variability properties of the two classes.

BL Lacs are more variable in the hard (0.7–8 keV) than in the soft (0.05–2 keV) X-ray band. This behavior has been noted by other authors (e.g., in PKS 2155−304 [Treves *et al.* 1989] and other BL Lacs [George, Warwick, and Bromage 1988; George, Warwick, and McHardy 1989]) and has been interpreted by George, Warwick, and McHardy (1989) within the framework of an inhomogeneous synchrotron self-Compton model. Our systematic analysis clearly shows that this phenomenon is very common among X–BL Lacs, since it is present in most, if not all, of the X–BL Lacs which have been found to be variable in this study. This result is not confined to *EXOSAT* data but is also supported by the comparison of simultaneous *Einstein* IPC and MPC data (Schwartz and Madejski 1986). The famous 30 s variability event seen in the *Einstein* light curve of H0323+022 was seen only in the high-energy channels of the IPC detector, while the 0.1–0.5 keV flux remained approximately constant (Feigelson *et al.* 1986). The opposite phenomenon, i.e., spectral *steepening* with increasing brightness, seems instead to be rather common in other types of AGN. Examples of sources exhibiting this behavior are PG 1211+143 (Elvis *et al.* 1989), NGC 4051 (Lawrence *et al.* 1985; Matsuoka *et al.* 1989), MCG 6-30-15 (Matsuoka *et al.* 1989), NGC 7314 (Turner 1989), NGC 5548 (Branduardi-Raymont 1986), NGC 6814 (Mittaz and Branduardi-Raymont 1989), and Fairall 9 (McHardy 1988).

The luminosity variability function of BL Lacs has been derived using LE data. The LVF is a steep function of variability amplitude, reflecting the fact that large-amplitude variations are rare, with sources spending half of their time within a factor of 2 of a quiescent level. Large variations are much more likely to have been observed in well-known, bright, and well-monitored objects, rather than in BL Lacs that are faint and only recently discovered. The fact that X–BL Lacs seem to have shown less dramatic optical variability and less polarization than classical radio-selected BL Lacs (Stocke *et al.* 1985) could simply be a direct consequence of the steep LVF. The large majority of the X–BL Lacs have only recently been discovered and have not been as extensively monitored as most of the famous and long-known Q–BL Lacs.

Rapid and large-amplitude flux variability, implying high efficiencies or special geometries of the emitting region, was observed in only one object (PKS 2155−304), with the possible addition of three others if their currently unknown redshifts are larger than the critical values derived above.

In a few cases an episode of rapid variability was completely observed from beginning to end, giving a proper measure of the time scales involved. These amounted to a minimum of ≈ 2 hr for Mrk 421, ≈ 5 hr for PKS 2155−304 and ≈ 15 hr for ON 325. The fact that the rise time of an event was approximately equal to decay time suggests that time scales are dictated by the size of the emitting region rather than by the physical acceleration and energy-loss mechanism.

The results of the analysis of LE data reveal no evidence for intrinsic absorption due to cold gas in excess of a few 10^{20} atoms cm^{-2}; this is in good agreement with several other results (e.g., Madejski and Schwartz 1989). In a few cases intrinsic absorption in BL Lac objects has been reported (Urry 1986). However, we note that high intrinsic absorption could be simulated by a decrease in intensity in the soft X-ray band caused by spectral curvature similar to that detected by *EXOSAT* in a number of objects (e.g., Barr *et al.* 1989*a*, *b*).

We thank G. Gavazzi for useful discussions and for pointing out the analogy between the radio luminosity function and the LVF, and G. Tagliaferri for providing some of the hard X-ray light curves of PKS 2155−304. We also wish to thank the referee for several useful suggestions.

REFERENCES

Bladwin, J. E. 1971, in *IAU Symposium 46, The Crab Nebula*, ed R. D. Davis and F. G. Smith (Dordrecht: Reidel), p. 22.
Barr, P., Giommi, P., and Maccagni, D. 1988, *Ap. J.* (*Letters*), **324**, L11.
Barr, P., *et al.* 1989*a*, in preparation.
Barr, P., Giommi, P., Pollock, A. M. T., Tagliaferri, G., Maccagni, D., and Garilli, B. 1989*b*, in *BL Lac Objects*, ed. L. Maraschi, T. Maccacaro, and M.-H. Ulrich (Berlin: Springer-Verlag), p. 290.
Borra, E. F., and Corriveau, G. 1984, *Ap. J.*, **276**, 15.
Bradt, H. V., Remillard, R. A., Tuohy, I. R., Buckely, D. A. H., Brissenden, R., Schwartz, D. A., and Roberts, W. 1988, in *The Physics of Neutron Stars and Black Holes*, ed. Y. Tanaka (Tokyo: Universal Academy Press), p. 527.
Branduardi-Raymont, G. 1986, in *The Physics of Accretion onto Compact Objects*, ed. K. O. Mason, M. G. Watson, and N. E. White (Berlin: Springer-Verlag), p. 407.
Bregman, J. N., *et al.* 1988, *Ap. J.*, **331**, 746.
———. 1990, *Ap. J.*, **325**, 574.
———. 1982, *Ap. J.*, **253**, 19.
Brindle, C., Hough, J. H., Bailey, J. A., Axon, D. J., and Hyland, A. R. 1986, *M.N.R.A.S.*, **221**, 739.
Brown, L. M. J, Robson, E. I., Gear, W. K., Crosthwaite, R. P., McHardy, I. M., Hanson, C. G., Geldzahler, B. J., and Webb, J. R. 1986, *M.N.R.A.S.*, **219**, 671.
Burbidge, G., and Hewitt, A. 1987, *Ap. J.*, **92**, 1.
Cavallo, G., and Rees, M. J. 1978, *M.N.R.A.S.*, **183**, 359.
Cruz-Gonzales, I., and Huchra, J. P. 1984, *A.J.*, **89**, 441.
Danzinger, I. J., Fosbury, R. A. E., Goss, M. N., and Ekers, R. D. 1979, *M.N.R.A.S.*, **188**, 415.
De Korte, P. A. J., *et al.* 1981, *Space Sci. Rev.*, **30**, 495.
Doxsey, R., Bradt, H., McClintock, J., Petro, L., Remillard, R., Ricker, G., Schwartz, D. A., and Wood, K. 1983, *Ap. J.* (*Letters*), **264**, L43.
Elvis, M., Giommi, P., McDowell, J., and Wilkes, B. 1989, *Bull AAS*, **20**, 1024.
Fabian, A. C., and Rees, M. J. 1979, in *IAU/COSPAR Symposium on X-ray Astronomy* (Innsbruck) (*Adv. Space Res.*, **3**, 381).
Falomo, R., Bouchet, P., Maraschi, L., Tanzi, E. G., and Treves, A. 1989, *Ap. J.*, **345**, 148.
Feigelson, E., *et al.* 1986, *Ap. J.*, **302**, 337.
George, I. M., Warwick, R. S., and Bromage, G. E. 1988, *M.N.R.A.S.*, **232**, 793.
George, I. M., Warwick, R. S., and McHardy, I. M. 1989, *M.N.R.A.S.*, in press.
Ghisellini, G., and Maraschi, L. 1989, *Ap. J.*, **340**, 181.
Ghisellini, G., Maraschi, L., Tanzi, E. G., and Treves, A. 1986, *Ap. J.*, **310**, 317.
Gioia, I. M., Maccacaro, T., Schild, R. E., Wolter A., Stocke, J. T., Morris, S. L., and Henry, J. P. 1990, *Ap. J. Suppl.*, **72**, 567.
Giommi, P. 1985, *The EXOSAT Express*, No. 12, p. 33.
Giommi, P., and Angelini, L. 1987, *The EXOSAT Express*, No. 18, p. 45.
Giommi, P., Barr, P., Garilli, B., Gioia, I. M., Maccacaro, T., Maccagni, D., and Schild, R. E. 1987, *Ap. J.*, **322**, 662.
Giommi, P., Barr, P., Gioia, I. M., Maccacaro, T., Schild, R. E., Garilli, B., and Maccagni, D. 1986, *Ap. J.*, **303**, 596.
Giommi, P., Beuermann, K., Barr, P., Schwope, A. Tagliaferri, G., and Thomas, H. C. 1989*b*, *M.N.R.A.S.*, **236**, 375.

Giommi, P., Tagliaferri, G., and Angelini, L. 1988, in *X-Ray Astronomy with EXOSAT* ed. N. E. White and R. Pallavicini (*Mem. Soc. Astr. Italiana* **59**, 33).
Giommi, P., *et al.* 1989*a*, in *BL Lac Objects*, ed. L. Maraschi, T. Maccacaro, and M.-H. Ulrich (Berlin Springer-Verlag), p. 231.
Griffiths R. E., Wilson A. S., Ward M. J., Tapia, S., and Ulvestad, J. S. 1989, *M.N.R.A.S.*, **240**, 33.
Halpern, J. P., Impey, C. D., Bothun, G. D., Tapia, S. Schillman, E. D., Wilson, A. S., and Meurs, E. J. A. 1986, *Ap. J.*, **302**, 711.
Hewitt, A., and Burbidge, G. 1987, *Ap. J. Suppl.*, **63**, 1.
Hummel, E. 1981, *Astr. Ap.*, **93**, 93.
Impey, C. D., and Brand, P. 1982, *M.N.R.A.S.*, **201**, 849.
Jannuzi, B., and Green, R. 1989, in *BL Lac Objects*, ed. L. Maraschi, T. Maccacaro, and M.-H. Ulrich (Berlin Springer-Verlag), p. 135.
Jones, T. W., Rudnick, L., Owen, F. N., Puschell, J. J., Ennis, D. J., and Werner, M. W. 1981, *Ap. J.*, **243**, 97.
Kinman, T. D. 1976, *Ap. J.*, **205**, 1.
Kuhr, H., Pauliny-Toth, I. I. K., Witzel, A., and Schmidt J. 1981, *A.J.*, **86**, 854.
Landau, R., Jones, J. W., Epstein, E. E., Neugebauer, G., Soifer, B. J., Werner, M. W., Puschell, J. J., and Balonek, J. J. 1983, *Ap. J.*, **268**, 68.
Landau, R., *et al.* 1986, *Ap. J.*, **308**, 78.
Lawrence, A., Watson, M. G., Pounds, K. A., and Elvis, M. 1985, *M.N.R.A.S.*, **217**, 685.
Ledden, J. E., and O'Dell, S. L. 1985, *Ap. J.*, **298**, 630.
Maccacaro, T., Gioia, I. M., Maccagni, D., and Stocke, J. T. 1984, *Ap. J. (Letters)*, **284**, L23.
Maccacaro, T., Gioia, I. M., Schild, R. E., Wolter, A., Morris, S. L., and Stocke, J. T. 1989, in *BL Lac Objects*, ed. L. Maraschi, T. Maccacaro, and M.-H. Ulrich (Berlin: Springer-Verlag), p. 222.
Maccagni, D., Garilli, B., Schild, R., and Tarenghi, M. 1987, *Astr. Ap.*, **178**, 21.
Madejski, G. M. 1985, Ph.D. thesis, Harvard University.
Madejski, G. M., and Schwartz, D. A. 1989, in *BL Lac Objects*, ed. L. Maraschi, T. Maccacaro, and M.-H. Ulrich (Berlin: Springer-Verlag), p. 267.
Maraschi, L., Ghisellini, G., Tanzi, E., and Treves, A. 1986, *Ap. J.*, **310**, 317.
Matsuoka, M., Yamauchi, M., Piro, L., and Murakami, T. 1989, *Ap. J.*, submitted.
McHardy, I. 1988, *Mem. Soc. Astr. Italiana*, **59**, 239.
Mittaz, J. P. D., and Branduardi-Raymont, G. 1989, *M.N.R.A.S.*, **238**, 1029.
Morini, M., Chiappetti, L., Maccagni, D., Maraschi, D., Tanzi, E. G., Treves, A., and Wolter, A. 1986, *Ap. J. (Letters)*, **306**, L71.
Mufson, S. L., *et al.* 1984, *Ap. J.*, **285**, 571.
Owen, F. N., Spangler, S. R., and Cotton, W. D. 1980, *A.J.*, **85**, 351.
Perley, R. A. 1982, *A.J.*, **87**, 859.
Pica, A. T., Pollock, J. T., Smith, A. G., Leacock, R. J., Edwards, P. L., and Scott, R. L. 1980, *A.J.*, **85**, 1442.
Piccinotti, G., Mushotzky, R. F., Boldt, E. A., Holt, S. S., Marshall, F. E., Serlemitsos, P. J., and Shafer, R. A. 1982, *Ap. J.*, **253**, 485.
Pollock A. M. T., *et al.* 1990, in preparation.
Puschell, J. J., and Stein, W. A. 1980, *Ap. J.*, **237**, 33.
Remillard, R. A., Tuohy, I. R., Brissenden, R. J. V., Buckley, D. A. H., Schwartz, D. A., Feigelson, E. D., and Tapia, S. 1989, *Ap. J.*, **345**, 140.
Schmitt J. 1986, *Nature*, **218**, 663.
Schwartz, D. A., Brissenden, R. J. V., Tuohy, I. R., Feigelson, E. D., Hertz, P. L., and Remillard, R. A. 1989, *Bull. AAS.*, **21**, 777.
Schwartz, D. A., and Madejski, G. M. 1986, in *Variability of Galactic and Extragalactic X-Ray Sources*, ed. A. Treves (Milan: Associazione per l'Avanzamento dell'Astronomia), p. 65.
Sitko, M. L., and Junkkarinen, V. T. 1985, *Pub. A.S.P.*, **97**, 1158.
Smith, A. G., Balonek, T. J., Elston, R., and Heckert, P. A. 1987, *Ap. J. Suppl.*, **64**, 459.
Stark, A., Heiles, C., Baily, and Linke, K. 1990, in preparation.
Staubert, R., Bazzano, A., Ubertini, P., Brunner, H., Collmar, W., and Kendziorra, E. 1986, *Astr. Ap.*, **162**, 16.
Staubert, R., Brunner, H., and Worrall, D. M. 1986, *Ap. J.*, **310**, 694.
Stein, W. A., O'Dell, S. L., and Strittmatter, P. A. 1976, *Ann. Rev. Astr. Ap.*, **14**, 173.
Stocke, J. T., Liebert, J., Schmidt, G., Gioia, I. M., Maccacaro, T., Schild, R. E., Maccagni, D., and Arp, H. 1985, *Ap. J.*, **298**, 619.
Stocke, J. T., Morris, S. L., Gioia, I. M., Maccacaro, T., Schild, R. E., and Wolter, A. 1988, in *Optical Surveys for Quasars*, ed. P. Osmer, A. C. Porter, R. Green, and C Foltz (San Francisco: Astronomical Society of the Pacific), p. 311.
———. 1990, *Ap. J.*, **348**, 141.
Tagliaferri, G., *et al.* 1989*a*, in *BL Lac Objects*, ed. L. Maraschi, T. Maccacaro, and M.-H. Ulrich (Berlin: Springer-Verlag), p. 257.
Tagliaferri, G., Stella, L., Maraschi, L., Treves, A., and Morini, M. 1989*b*, in *BL Lac Objects* ed. L. Maraschi, T. Maccacaro, and M.-H, Ulrich (Berlin Springer-Verlag), p. 314.
Tranzi, E. G., Falomo, R., Bouchet, P., Bersanelli, M., Maraschi, L., and Treves, A. 1989, in *BL Lac Objects*, ed. L. Maraschi, T. Maccacaro, and M.-H. Ulrich (Berlin: Springer-Verlag), p. 171.
Taylor, B. G., Andersen, R. D., Peacock, A., and Zobl, R. 1981, *Space Sci. Rev.*, **30**, 479.
Treves, A., *et al.* 1989, *Ap. J.*, **341**, 733.
Trümper, J. 1984, in *X-Ray and UV Emission from Active Galactic Nuclei*, ed. W. Brinkmann and J. Trümper (Garching: MPE), p. 254.
Turner, M. J. L., Smith, A., and Zimmermann, H. U. 1981, *Space Sci. Rev.*, **30**, 513.
Turner, T. J. 1989, *M.N.R.A.S.*, **226**, 9P.
Ulmer, M. P., Brown, R. L., Schwartz, D. A., Patterson, J., and Cruddace, R. G. 1983, *Ap. J.*, **270**, L1.
Ulvestad, J. S., Johnston, K. J., and Weiler, K. W. 1983, *Ap. J.*, **266**, 18.
Urry, C. M. 1986, in *The Physics of Compact Objects*, ed. K. O. Mason and N. E. White (Berlin: Springer-Verlag), p. 357.
Véron-Cetty, M. P., and Véron, P. 1985, *ESO Sci. Rept.*, No. 4
Wall, J. V., Shimmins, A. J., and Bolton, J. G. 1975, *Australian J. Phys. Ap. Suppl.*, **34**, 55.
Weiler, K. W., and Johnston, K. J. 1980, *M.N.R.A.S.*, **190**, 269.
White, N. E., and Peacock, A. 1988, in *X-Ray Astronomy with EXOSAT*, ed. N. E. White and R. Pallavicini (*Mem. Soc. Astr. Italiana*, **59**, 7).
Worrall, D. M. 1989, in *BL Lac Objects*, ed. L. Maraschi, T. Maccacaro, and M.-H. Ulrich (Berlin: Springer-Verlag), p. 305.
Worrall, D. M., *et al.* 1984*b*, *Ap. J.*, **284**, 512.
Worrall, D. M., Giommi, P., Tananbaum, H., and Zamorani, G. 1987, *Ap. J.*, **313**, 596.
Worrall, D. M., Puschell, J. J., Rodriguez-Espinosa, J. M., Bruhweiler, F. C., Miller, H. R., Aller, M. F., and Aller, H. D. 1984*a*, *Ap. J.*, **286**, 711.

P. Barr, P. Giommi, and A. M. T. Pollock: *EXOSAT* Observatory, Astrophysics Division, Space Science Department of ESA, Keplerlaan 1, 2200 AG Noordwijk, The Netherlands

B. Garilli and D. Maccagni: Istituto di Fisica Cosmica del CNR, Via Bassini 15, 20133 Milano, Italy